Title

Thermal stress responses of the antipatharian *Stichopathes sp.* from the mesophotic reef of Mo'orea, French Polynesia

Authors

Mathilde Godefroid[1], Laetitia Hédouin[2,3], Alexandre Mercière[2,3], Under The Pole Consortium[4], Philippe Dubois[1]

Affiliations

[1]Laboratoire de Biologie marine, Université Libre de Bruxelles, Avenue F.D. Roosevelt 50, CP160/15, 1050 Bruxelles, Belgium

[2]PSL Research University: EPHE-CNRS-UPVD, USR 3278 CRIOBE, BP 1013, 98729 Papetoai, Mo'orea, French Polynesia

[3]Laboratoire d'Excellence « CORAIL», Mo'orea, French Polynesia

[4]Under The Pole, 29900 Concarneau, France

Corresponding author

Mathilde Godefroid, mathilde.an.godefroid@ulb.be

Abstract

Antipatharians, also called black corals, are present in almost all oceans of the world, until extreme depths. In several regions, they aggregate in higher densities to form black coral beds that support diverse animal communities and create biodiversity hotspots. These recently discovered ecosystems are currently threatened by fishing activities and illegal harvesting for commercial purposes. Despite

Highlights (for review : 3 to 5 bullet points (maximum 85 characters including spaces per bullet point)

Highlights

- Metabolic performances of *Stichopathes sp.* are optimal at 28.3°C (T_{opt})
- *Stichopathes sp.* lives at suboptimal performances during the cold season
- *Stichopathes sp.* has low acclimatization capacity and a narrow thermal breadth
- Exceeding of T_{opt} has significant consequences for *Stichopathes sp.*
- Exceeding of T_{opt} could occur with a 1°C increase during the colder months

Graphical Abstract

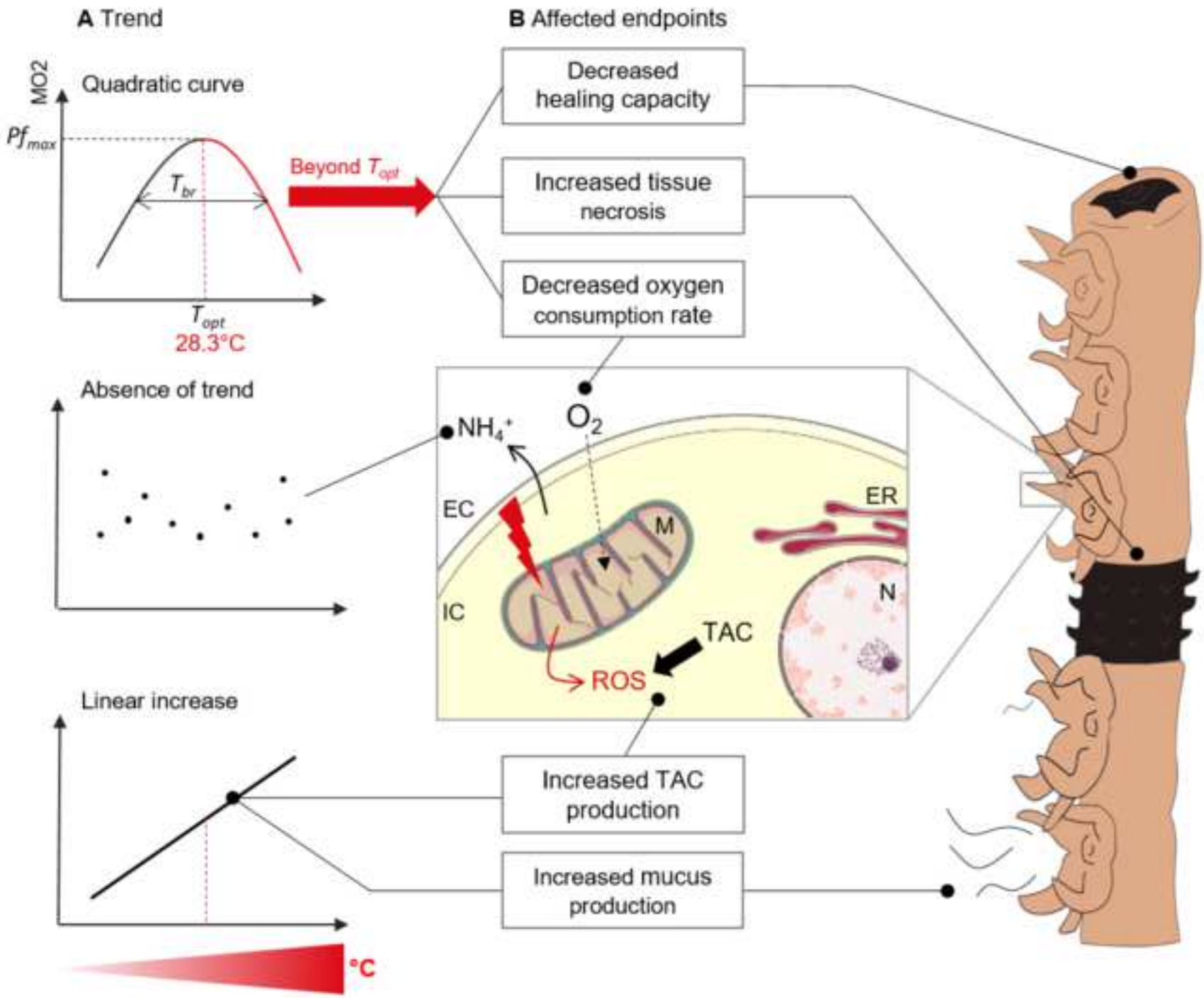

this, studies dedicated to the physiology of antipatharians are scarce and their responses to global change stressors have remained hardly explored since recently. Here, we present the first study on the physiological responses of a mesophotic antipatharian *Stichopathes sp.* (70-90 m) to thermal stress through a 16-d laboratory exposure (from 26 to 30.5°C). Oxygen consumption measurements allowed identifying the physiological tipping point of *Stichopathes sp.* (T_{opt} = 28.3°C; 2.7°C above mean ambient condition). Our results follow theoretical predictions as performances start to decrease beyond T_{opt}, with lowered oxygen consumption rates, impairment of the healing capacities, increased probability of tissue necrosis and stress responses activated as a function of temperature (*i.e.* increase in mucocyte density and total antioxidant capacity). Altogether, our work indicates that *Stichopathes sp.* lives at suboptimal performances during the coldest months of the year, but also that it is likely to have low acclimatization capacity and a narrow thermal breadth.

Keywords

Thermal performance, Eco-physiology, Mesophotic, Antipatharians, Heat stress, *Stichopathes sp.*

1. Introduction

Tropical coral reefs are at a critical tipping point. Oceans have warmed from the surface to the deep sea (Hughes & Narayanaswamy, 2013; Levin & Le Bris, 2015; Sweetman et al., 2017; Yasuhara & Danovaro, 2016; IPCC, 2018), due to increasing anthropogenic greenhouse gases emissions in the atmosphere. Based on the most pessimistic emission scenario (RCP 8.5), climate model projections forecast an increase in sea surface temperature relative to 1850-1900 up to 4.3°C (3.2-5.4) for the end of the century (IPCC, 2019). In particular, coral reefs have received much attention this last decade due to the increasing intensity and frequency of bleaching events, and the subsequent unprecedented mortality. As a consequence, shift in coral reef composition may occur, with reef landscapes being

dominated by algae (as exemplified by the Caribbean area; Antonius & Ballesteros, 1998) instead of corals, which seriously questions the future of coral reefs and their associated socio-ecological services. Depth can attenuate the physical magnitude of some stressors (such as temperature anomalies and storm events, reviewed by Smith et al., 2019), that are increasingly affecting shallow-water ecosystems (Bongaerts et al., 2010). Therefore, it was suggested that ecosystems located at mesophotic depths (30-150 m; Mesophotic coral ecosystems, MCEs) may act as refugia from many local and global anthropogenic impacts (Bongaerts et al., 2010, 2017 ; Glynn, 1996; Thomas et al., 2015; Lindfield et al. 2016). However, the impacts of disturbances over depth are often not straightforward and can vary spatially and temporally (Smith et al., 2016). In particular, heat stress exposure does not decline reliably with depth (as modelled by Schramek et al., 2018; Venegas et al., 2019) and does not necessarily decrease with depth, due to physical forcing (Bridge et al., 2013; Frade et al., 2018; Leichter et al., 2006; Neal et al., 2014; Rocha et al., 2018; Smith et al., 2019).

Nonetheless, our understanding of coral reef ecosystems is biased by the preponderance of data from depths above 30 m, which represents less than one-fifth of the total depth range of the tropical coral reef environment (Pyle et al., 2016). How coral reef ecosystems are able to deal with climate change in deeper areas remains relatively unexplored. Mesophotic reefs also harbour unique landscapes, with scleractinian corals but also non-scleractinian anthozoa such as gorgonians, antipatharians and alcyonacea that play key roles in this zone, and sometimes even dominate over scleractinian corals (Bo et al., 2014). It is only recently that studies have started to focus on how non-scleractinian and scleractinian corals of the mesophotic zone cope with climate changes and their role in the coral reef functioning. It is clear that based on the available data from mesophotic reefs, an understanding of all components of MCEs is essential to successfully characterize the health of coral reefs in general (Pyle et al., 2016). Despite our knowledge about the great potential of hidden biodiversity and the important ecological role of non-scleractinian corals of the mesophotic zone for the broader marine ecosystems, our understanding of how non-scleractinian corals of the mesophotic zone respond to climate change remains relatively unexplored. This is particularly true for antipatharians, the so-called black corals.

Antipatharians is one of the taxa for which the effects of heat stress remain uninvestigated, despite studies showing the importance of temperature in their bathymetric and geographic distribution (Bo et al., 2008; Wagner, 2015; Yesson et al., 2017). Antipatharians are present in almost all oceans of the world (up to 8600 m depth; Molodtsova, 2008; Wagner et al., 2012), with abundance increasing with depth (75% of described species below 50 m, Wagner et al., 2012) and reaching a peak at mesophotic depths. There, they often live as isolated colonies but they can also form dense assemblage under the right conditions (Bo et al., 2019; Cairns, 2007), and form the so-called “black coral forests” (Orejas & Jiménez, 2017; Rossi et al., 2017). These forests provide major three-dimensional habitats associated with highly diverse fauna and acting as spawning, nursery and feeding areas for many species (Bo et al., 2019; De Assis et al., 2019; De Clippele et al., 2019; Suarez et al., 2015; Tazioli et al., 2007; Wagner et al., 2012). The skeleton of antipatharians is made of chitin and proteins (Goldberg, 1978; Goldberg, 1994; Juárez-de la Rosa et al., 2012; Kim et al., 1992) and is sought to be used for medical, religious or decorative purposes, or sold as precious corals in the jewellery trade in several regions across the globe (Bruckner et al., 2008; Bruckner, 2016; Grigg, 2001; Tsounis et al., 2010; Todinanahary et al., 2016). Diverse microbial communities were described within and around antipatharian tissues (Dannenberg et al., 2015; Liu et al., 2018; Penn et al., 2006; Santiago-Vázquez et al., 2007; van de Water et al., 2020; Zhang et al., 2012). They are known to play significant roles in antipatharian health, and may be a key player for acclimatization and/or adaptation to future environmental changes (Bosch & McFall-Ngai, 2011; McFall-Ngai et al., 2013; van de Water et al., 2020). While antipatharians have long been referred to as azooxanthellate species, recent studies have shown the presence of *Symbiodiniaceae* within the tissues of various families of antipatharians (*Antipathidae*, *Aphanipathidae*, *Myriopathidae* and *Schizopathidae*; Bo et al., 2011; Wagner et al., 2011). Although the role of symbiosis in the physiology and energetics of antipatharians remains hardly explored, it is suggested to be limited or absent (Gress et al., 2021; Wagner et al., 2011). In the present work, the term “antipatharian” will always implicitly refers to the black coral holobiont, which include the host antipatharian and all microorganisms living within and around the host.

The ultimate impacts of heat stress on organisms and ecosystems will depend both on the *magnitude* of the stress (and its possible variations) and on the *susceptibility* of the impacted organism/ecosystem (its *resistance* to the stress and potential for *recovery* following the stress; Battisti et al., 2016; Bongaerts & Smith, 2019; Holling, 1973; Smith et al., 2019). At mesophotic depths, the magnitude of the stress may be dampened as compared to shallow waters but adaptation or long-term acclimatization to local conditions may result in increased susceptibility (Smith et al., 2016). In particular, benthic organisms such as corals are expected to be particularly sensitive to heat stress (Hughes et al., 2017; Spalding & Brown, 2015). Unable to move into cooler waters, they will depend in the first instance on physiological adjustments followed in the longer term by adaptive changes (Solan & Whiteley, 2016). The measurement of physiological rates enables the quantification of energy expenditure in biological systems and provide insight to organism health. It relies on the idea that most physiological functions, such as metabolism, locomotion and growth, perform optimally at a specific temperature (T_{opt}, the optimal temperature, when performances are maximal; Payne et al., 2016; Angiletta et al., 2009), around which their performances start to decrease due to the progressive loss of oxygen supply to tissues (Dell et al., 2013; Portner, 2010; Schulte, 2015). This concept defines a thermal window of performance that matches the window of aerobic scope in water breathers (Pörtner, 2010). Thermal sensitivity can be understood by measuring the rates of various physiological functions over a temperature gradient, usually in the form of a thermal performance curve (TPC; Huey & Stevenson, 1979; Jurriaans & Hoogenboom, 2020). The typical shape of a TPC describes the increase of performance with temperature up to a maximum (Pf_{max}) occurring at a specific temperature (T_{opt}) followed by the decline in performance around T_{opt}. The thermal breadth of the curve (T_{br}) corresponds to the thermal window of performance of the organism. The capacity of an organism/taxa to change the shape (T_{opt} and T_{br}) of the TPC (*i.e.* its plasticity of thermal performances), through physiological acclimatization, provides insight into its capacity to adapt and acclimatize to ocean warming (Logan et al., 2014).

It is usually expected that the shape of TPC in ectotherms will reflect the range of temperatures that they experience in the environment (as in Deutsch et al., 2008; Frazier et al., 2006; Huey & Stevenson, 1979), as ectotherms acclimatize (phenotypically) and adapt (genetically) to different temperatures (Angilletta, 2009). Despite this, temperatures that maximize the physiological performances of ectotherms in the lab are often different from the temperature at which they prefer to operate in the environment (Martin & Huey, 2008), which complicates the understanding of the impact of warming on ectotherms (Payne et al., 2016). So, due to adaptive differences among taxa and various types of plasticity such as epigenetic effects, developmental plasticity and acclimatization, there is an enormous amount of variation in TPC among taxa (Dell et al., 2011; Schulte, 2015; Schulte et al., 2011). If we are willing to predict ecosystem-level effects of global change, it is first required to understand the resilience of each taxa independently.

To fill the gap of knowledge on antipatharian sensibility to climate change, we provided here the first assessment on the susceptibility of an antipatharian to heat stress, by working on the mesophotic (90 m) whip antipatharian *Stichopathes sp.* from Mo'orea (French Polynesia). This work aimed at assessing the thermal performances of *Stichopathes sp.* and understanding its physiological capability to cope with environmental change. For this purpose, we selected a set of endpoints that are relevant to understand the metabolic state and stress-level of the organism. In particular, we looked at the rates of oxygen consumption and nitrogen excretion, as well as the capacity of *Stichopathes sp.* to heal under distinct treatments (+1.5, +3 and +4.5°C). We hypothesized that this range of temperatures will allow us to identify the physiological "tipping point" (T_{opt}) of *Stichopathes sp.*, and that other measured endpoints will also follow a bell-shaped performance curve. We also looked at O:N ratios to detect a potential change in the metabolic substrate used (protein/amino acids *vs* lipids/carbohydrates; Mayzaud & Conover, 1988), expecting to witness a metabolic shift to deal with challenging environmental conditions. Finally, we measured mucocyte density and tissue necrosis as stress indicators, and quantified the total antioxidant capacity (TAC) of *Stichopathes sp.* as a measure of

cellular stress level. Here, we hypothesized that stress will increase linearly with temperature, as commonly observed in stress responses.

2. Material and methods

2.1 Sampling site and antipatharian collection

While the presence of antipatharians around the island of Mo'orea is known by recreational divers, no scientific census has been carried out so far. Therefore, we focused on a specific site in the outer reef of North of Mo'orea (French Polynesia, 17° 28' 41.7'' S, 149° 51' 09.9'' W). Sampling was carried out by technical divers from "Under the Pole" expeditions (https://www.underthepole.com/). Temperature sensors (HOBO Water Temperature Pro V2 Data logger, Onset Computer Corporation, MA, USA) were installed at 6, 20, 40, 60 and 90 m on October 9th 2019, and recovered on November 17th 2019.

All the colonies of *Stichopathes sp.* used in the experiment (N=38) were collected between 70 and 90 m depth in a single dive on October 18th 2019, following the local legislation for antipatharian collection. Due to the difficulty to discriminate *Stichopathes* species based solely on macro-morphological features *in situ*, associated with the lack of knowledge on *Stichopathes* species in French Polynesia, the most abundant morphotype of *Stichopathes sp.* was sampled. The morphotype is characterized by an orange-brown corallum, straight to sinuous, which can make few irregular coils (Figure 1a). Polyps form one row along the stem, with some turning around certain portions of the stem, in an irregular manner. The polyps are paler than the rest of the coenenchyma (Figure 1b). Their transverse diameter is around 1-1.5 mm and interpolypar space is null. Colonies ranged in length from 20 to 40 cm. Preliminary analyses carried out on NAD2 mitochondrial gene showed that all specimens belonged to a single species and suggested the closest species to be *Stichopathes cf. occidentalis* (Gray, 1860), based on currently available data.

175 Just after collection by the deep rebreather divers, colonies were brought to the surface with a surface
176 marker buoy to be recovered by a boat and directly installed in aquaria maintained at the temperature
177 of the collection site (~26°C). They were then left to recover from the sampling stress for three days
178 prior to fragmentation, in the aquarium facilities of the CRIOBE (Centre de Recherches Insulaires et
179 Observatoire de l'Environnement). This duration was considered sufficient based on morphological
180 and behavioural observations of the colonies (polyp extension and feeding at night, absence of mucus
181 production).

182 ***2.2 Experimental design***

183 The experiment was carried out in five 200L-aquaria with flow-through seawater (seawater
184 parameters, Table 1), under *in situ* light conditions at 90 m (4-15 µmol m^{-2} s^{-1}). Four temperature
185 treatments (26°C, control temperature, two tanks; 27.5°C; 29°C and 30.5°C) were maintained for 16
186 days. The seawater was sand and UV filtered before entering each aquarium and temperature was
187 controlled using chillers (TECO TK500, Italy).

188 Due to the difficulty of collecting mesophotic *Stichopathes sp.* from 70 to 90 m, the design of the
189 experiment was adapted to the availability of the colonies. In total, 38 colonies were used in the
190 experiment. Eight colonies were used to assess the healing capacity on a daily basis and to collect
191 samples for histological analyses at day 16. Among those, 6 colonies were cut into 5 nubbins (1 per
192 aquarium) and 2 colonies into 4 nubbins (1 per aquarium, but one), with a total of 7-8 nubbins of 6.91
193 ± 0.19 cm (mean ± se, n=38) per aquarium. The 30 remaining colonies were used for the respiration
194 rate and ammonium excretion rate measurements (6 different colonies per aquarium). The irregularly
195 sinuous corallum of *Stichopathes sp.* made it impossible to fit the whole colony in the respirometry
196 chamber without touching its walls and creating stress. Therefore, each colony was cut in three
197 nubbins of similar size (5.32 ± 0.08 cm, mean ± se, n=90). In total, 25-26 nubbins were held per
198 aquarium (7-8 for healing capacity observations and 18 for respirometry measurements). They were
199 fixed to vertical plastic holders by plastic cable ties.

Nubbins were maintained for two weeks after fragmentation at collection site temperature (26°C). Then, temperature was gradually increased in the aquaria by 0.5°C per day until reaching their respective target temperatures. At every stage since collection, corals were fed with a mix composed of freshly hatched *Artemia salina*, thawed copepods and plankton at around 7 PM every night.

2.3 Seawater parameters control and measurements

Temperature in each aquarium was controlled independently using TK500 chillers (Teco, Italy). Temperature and salinity were measured daily using a certified thermometer (VWR traceable digital thermometer with probe, VWR International, LLC) and a conductivity meter equipped with a conductivity electrode (Mettler-Toledo, Switzerland), respectively. One temperature recorder was installed per aquarium (HOBO Pendant Temperature/Light Data Logger, Onset Computer Corporation, USA) for the duration of the experiment. pH was measured daily on the total scale (pH_T) in the aquaria using a portable pH meter (Metrohm, Switzerland) mounted with a standard pH probe that was calibrated every few days with Tris/AMP buffer (after Dickson et al., 2007). Measurements of total alkalinity (A_T) in seawater were made the same day of seawater collection in triplicate (50 mL each) every 2-3 days using open-cell potentiometric titration with an automated titrator (T50, Mettler-Toledo, Switzerland). Titrations of certified reference material (CRM) provided by A. G. Dickson (batch 171) were performed before each set of titration and the deviation from the nominal value (2217.40 ± 0.63 µmol kg^{-1}) was always below 5%. Mean seawater parameters are summarized in Table 1.

2.4 Response variables

2.4.1 Oxygen consumption rate

Standard metabolic rate (SMR) was estimated from rates of oxygen uptake using intermittent-flow respirometry (Clark et al., 2013) at the start of the experiment (day 0), 8 and 16 days after exposure to the heat treatments. The respirometry setup consisted of four cylindrical glass respirometry chambers (0.033-0.0035 L, including tubes and pumps), connected to a peristaltic pump system that circulated water in a closed circuit and a pump system that flushed the chambers at regular intervals (open

circuit). Oxygen Flow-Through Cell with an integrated oxygen sensor (OXFTC; Pyro Science GmbH, Aachen, Germany) were connected with tubes to each chamber (n=4) and to optic fibers to an optical oxygen meter (FireSting O2 (FSO2-C4); Pyro Science GmbH, Aachen, Germany). Respiration rate was measured on the three nubbins from the same colony simultaneously, placed in the same respirometry chamber, and results obtained per chamber were considered as single measurement. Oxygen concentration was recorded every 5 s using the software Pyro Oxygen Logger. The chambers were submersed in a temperature-controlled water bath (Tetra HT submersible heater) filled with filtered seawater (0.2 µm) with a recirculating pump that ensured the homogenisation of the temperature. A timer was used (NI-9481; National Instruments, Austin, TX, USA) to control the pump system. It combines (1) measurement periods (30 min) in a recirculating, but closed, respirometer, punctuated by (2) clean and fully-aerated water flush periods (3 min) which are long enough to ensure that the water is thoroughly exchanged to eliminate potential nitrogenous waste buildup in the chambers (Forstner, 1983; Steffensen, 1989; Svendsen et al., 2016).

Respirometry trials generally started around 7 AM, allowing a minimum of 12hrs of digestion after the last feeding. For each respiration trial, four chambers were used, three were filled up with three nubbins of the same colony and the last chamber was left empty with just seawater to serve as a control for background (microbial) respiration (Rodgers et al., 2016). The nubbins were left for one hour inside the chamber at the desired temperature before starting the measurements (3 cycles of 3 min/30 min), to allow them to recover from the stress of handling and acclimate to their new environment. At the end of the measurements, the nubbins were removed from their chambers and the oxygen uptake with empty chambers was measured for three other cycles, to account for the increase of bacterial metabolism over the course of the experiment, in each chamber independently. All the equipment and circulation system was sterilized (bleached) and filled with new filtered seawater (0.2 µm) between consecutive trials to keep background respiration low. SMR was calculated from the slope of the regression line of the oxygen concentration against time and normalized using the coral surface area, considered as a cylinder.

2.4.2 Ammonium excretion rate and O:N ratios

At the end of each respirometry trials and just before the start of the last flush, the circulation system was paused and 10-12 mL of seawater were collected in the chambers, filtered (0.2 µm) and freezed (-20°C). Ammonium concentration was determined using segmented flow nutrient analyser (QuAAtro, SEAL Analytical Inc., Germany) with minimum detectable value of 0.32 µM, using ammonium sulfate $(NH_4)_2SO_4$ as standard (r^2=0.99). The concentration in the chambers was corrected with the value measured in the control chamber and normalized using the coral surface area. All measured values of ammonium concentration were above the detection limit (>0.32 µM). However, changes in ammonium concentration from coral excretion in incubation chambers were not consistently higher than changes in control chambers from microbial activity, which led to calculations of negative values of ammonium concentration in multiple experimental chambers. When occurring, these concentrations were set to zero.

The O:N ratio (ratio between the atoms of oxygen consumed per atom of nitrogen excreted) was calculated for each nubbin at each experimental temperature using the equation:

$$O{:}N = \frac{(2\ MO_2)}{(NH_4^+)}$$

Where MO_2 is the oxygen consumption of the nubbin (in µmol h^{-1} cm^{-2}) and NH_4^+ is the ammonium excretion of the nubbin (same unit). It indicates the proportion of protein/amino acids *vs* lipids/carbohydrates that are being catabolized for the energy requirements, allowing to detect potential changes in the metabolic substrates used (Mayzaud & Conover, 1988).

2.4.3 Healing capacity

At day 0, the apical part of 7-8 nubbins per aquarium was cut to reveal their skeleton. Healing process of black coral tips was monitored by daily photographs of each nubbin under each treatment. A qualitative healing index (HI) was established to characterize the evolution of the healing process (Figure 1c). The HI goes from -1 (tissue necrosis, when more skeleton is visible than at day 1) to HI 5

(Complete healing and budding of a new apical polyp) and it encompasses HI 0 (State at day 1), HI 1 (>10% of the skeleton is covered by new tissues), HI 2 (10-75%), HI 3 (>75%) and HI 4 (100%).

2.4.4 Tissue necrosis

Tissue necrosis was assessed visually on all nubbins on a daily basis and reported as 0 (absence of necrosis) or 1 (presence of necrosis). Tissue necrosis was defined as the partial loss of living tissue on coral surface area, thus revealing the black skeleton beneath the tissues (HI -1, Figure 1c). Tissue necrosis is distinct from mortality as (1) it is a localized process, (2) nubbins were still able to feed (tentacles expansion at night) and (3) recovery is possible from partial loss (personal observation). Total mortality (tissue loss, absence of tentacles expansion at night, establishment of microalgae on the skeleton) was not observed in any treatment.

2.4.5 Mucocyte density

Coral polyp tissues were collected with a scalpel on 7-8 nubbins per aquarium on day 16. They were first preserved in buffered formaldehyde 10% for 48 hours and then dehydrated following multiple ethanol baths. The polyp tissues were embedded in paraffin blocks and oriented so that the tentacles of the polyp were cut transversally. Eight µm thick sections were cut and stained using Masson's trichrome. Photographs of the transversally cut tentacles were made (minimum of four tentacles per nubbin) using a microscope (ZEISS Axioscope A1, Germany) mounted with a camera (ZEISS Axiocam 305 color, Germany). Following this, a minimum of two zones per section were selected to evaluate the proportion of mucocytes per surface, using the software ImageJ (Schneider et al., 2012).

2.4.6 Biochemical biomarkers

At the end of the experimental treatments, 8 to 9 coral fragments of about 1 cm in length were randomly selected in each treatment. The tissues were separated from the skeletal fraction using a scalpel, moved into a tube with 200 µL of phosphate buffer (50 mM) and immediately stored at -80°C. Homogenates were made on ice using a micro tube homogenizer system with disposable pestles and

centrifuged for 10 min at 4°C (10000 x g). The supernatant was transferred to a new tube and stored at -80°C until biomarkers analyses.

Total protein content in the samples was determined using a commercial reagent kit based on the Bradford assay (Pierce™ BCA Protein Assay Kit, ThermoFisher Scientific Inc., USA) with bovine serum albumin (BSA) as standard (2 mg/mL). Protein contents were used for biomarker normalization. Measurement of total antioxidant capacity (TAC) was performed using OxiSelect™ Total Antioxidant Capacity Assay Kit (Cell Biolabs Inc., USA). It is an electron-transfer based assay (Huang et al., 2005) that measures the capacity of an antioxidant (here, Uric Acid) in the reduction of an oxidant (here, Copper (II) is reduced into Copper (I)). The degree of colour change is correlated with the sample's antioxidant concentrations. Absorbance was measured at 490 nm in a microplate reader (Epoch 2 Microplate Spectrophotometer, BioTek Inc., USA) and compared to uric acid standard curves. Results were normalized to the protein content and expressed as "mM Copper Reducing Equivalents per g of protein".

2.5 Data analysis

The respiration rates in each temperature treatment were analysed at day 8 and 16 using least square regression in the form of a second order polynomial: $y = ax^2 + bx + c$. The respiration rate was used as the dependent variable (n=6 nubbins per aquarium, 12 nubbins in the control) and temperature as the independent variable (n=4). The tipping point temperature (maximum x-value) of the polynomial was calculated using the formula:

$$x = \frac{-b}{2a} \text{ (first derivative = 0)}$$

To assess the effect of temperature on oxygen consumption, the temperature quotient Q_{10} (*i.e.* the proportional change of respiration in response to a temperature increase of 10°C) was calculated between consecutive temperatures, using the van't Hoff equation:

322 $$Q_{10} = \left(\frac{R_2}{R_1}\right)^{\left[\frac{10}{T_2 - T_1}\right]}$$

323 where R_1 and R_2 are the rates of oxygen consumption corresponding to low temperature (T_1) and high
324 temperature (T_2), respectively. Q_{10} values could not be calculated for each individual colony between
325 consecutive temperatures because different colonies were used at each temperature. Consequently,
326 they were calculated for the population to determine whether the respiration rates exhibit typical
327 thermochemical reaction effects or whether they were compensating for temperature.

328 The effect of temperature on ammonium excretion rates, O:N ratio and biochemical biomarkers (at
329 day 16) were analysed using simple linear regression ($y = ax + b$), with temperature as the
330 independent variable (n=4). Results for mucocyte tissue density were analysed similarly (data averaged
331 by nubbin). Polynomial regression was also performed for this parameter but the quadratic term (x^2)
332 was not significant.

333 The healing capacity under each experimental treatment was assessed looking at the evolution of the
334 healing index through time. Each day, the healing index of the eight nubbins at each temperature was
335 averaged. Healing index equal -1 were not considered and the two control aquaria were pooled in the
336 analyses. Data were analysed using nonlinear regressions (ordinal logistic regressions) following the
337 equation:

338 $$y = \frac{\alpha}{1 + e^{-\beta(x-\gamma)}}$$

339

340 Significant differences between the parameters α, β and γ were defined as non-overlapping 95%
341 confidence intervals.
342 The effect of temperature on tissue necrosis was evaluated using Kaplan-Meier estimate of survival
343 (*survfit*, *survival*, Therneau 2015a) and Cox-proportional hazard model (*coxme*, Therneau 2015b), due
344 to the binary nature of these data. This statistic estimates the probability that a nubbin will not show
345 loss of tissues past a particular day.

Analysis of residuals was carried out for all regression analysis. No trend in residuals was evidenced. All statistical analyses were performed using SYSTAT v13.2 (Systat Software, San Jose, CA), except for the analyses of oxygen consumption that were analysed using R (R Development Core Team 2017). Figures were made using both softwares.

3. Results

3.1 In situ thermal environment

Based on data from 2015 to 2021 available from SNO CRIOBE, the mean difference between warm and cold season temperatures was 2.7°C in surface waters (3 m) and decreased with depth down to 1.9°C at 50 m. Annual lowest temperatures were recorded in September and warmest temperatures in April (Figure 2a). Over the 40 days (October-November 2019) of *in situ* data collection along the outer reef slope north of Mo'orea, the temperature decreased with depth (Figure 2b), with an average temperature of 27.4 ± 0.02°C (mean ± se, n=11520) at 6 m down to 25.6 ± 0.03 °C (mean ± se, n=11520) at 90 m (Figure 2e). Data collected at 5-min intervals revealed the occurrence of short-term and high-amplitude temperature fluctuations (*i.e.* internal waves) from 60 m depth (Figure 2c). The intensity and frequency of internal waves increased with depth (Figure 2d) with mean daily temperature fluctuations of 0.2°C at 20 m *vs* 0.4°C at 90 m (Figure 2e). Accordingly, the full range of temperature observed over 40 days also increased with depth, with a temperature difference of 4.6°C measured at 90 m between the highest and lowest values (separated by a time period of 24 days) *vs* 2.9°C at 20 m (Figure 2e).

3.2 Metabolic and biochemical responses to heat stress

The relationship between respiration rate and temperature was successfully described by a quadratic equation, both after 8 and 16 days of exposure (Figure 3a-b; Supplementary Table S1). The optimal temperature for aerobic scope was 28.7°C and 28.3°C after 8 and 16 days of heat stress, respectively. At T_{opt}, respiration rates after 8 days ($MO2_{opt}$= 0.096 µmol cm^{-2} h^{-1}, 95% confidence intervals: 0.077-

371 0.115) and 16 days ($MO2_{opt}$= 0.102 µmol cm^{-2} h^{-1}, 95% confidence intervals: 0.082-0.121) did not differ
372 significantly. All Q_{10} values for respiration were outside the range of 2-3, typical for thermochemical
373 enzymatic reactions (Table 2). Q_{10} values at day 8 and in the lower part of the temperature range at
374 day 16 were under-compensated, while Q_{10} between 27.5 and 29°C at day 16 were reduced, indicating
375 over-compensation.

376 Coral ammonium excretion rates ranged from 0 to 0.44 µmol cm^{-2} d^{-1} and 0 to 0.86 µmol cm^{-2} d^{-1} after
377 8 and 16 days, respectively (Figure 3c-d). Coral excretion rates did not significantly relate to
378 temperature (Linear regression, *p=0.48* and *p=0.59*, after, respectively, 8 and 16 days; Supplementary
379 Table S2).

380 No significant trend between O:N ratio and temperature was evidenced (linear regressions, *p=0.66* and
381 *p=0.32*, after 8 and 16 days, respectively; Supplementary Table S3; Figure 2e-f). The overall mean
382 values were 55.03 ± 20.79 (mean ± se, n=22) and 77.76 ± 16.97 (mean ± se, n=21) after 8 and 16 days,
383 respectively.

384 Temperature affected the healing capacity of the nubbins depending on the exposure duration and
385 the treatment intensity (Figure 4; Supplementary Table S4). From 26 to 29°C, the maximum healing
386 index reached (α) did not differ significantly (based on the 95% CI of this parameter). At 30.5°C, this
387 maximum was significantly lower than at 26 to 29°C. The time needed to reach the 50% healing index
388 (γ) was significantly shorter at 27.5 than at 29°C (3.4 days *vs* 3.9 days, respectively) and both were
389 significantly shorter than at 26°C (5.2 days). Finally, the healing rate (β) is significantly faster at 27.5°C
390 than at 26°C but not at 29°C. The time to reach the 50% healing index and the healing rate at the three
391 lower temperature treatments were not compared with the 30.5°C treatment as nubbins under the
392 latter healed faster but never reached a thorough healing.

393 Survival curves showing the appearance of tissue necrosis with time revealed an increased loss of
394 tissue at 29 and 30.5°C related to control conditions (Cox Proportional Hazards Models, *p=0.003* and

395 *p<0.001*, respectively; Figure 5; Supplementary Tables S5 and S6). No differences were highlighted at
396 27.5°C compared to 26°C (*p=0.41*).

397 After 16 days, the surface occupied by mucocytes on histological sections increased linearly with
398 temperature and the cells appeared enlarged at higher temperatures (Linear regression, *p<0.001*;
399 Figure 6a, see Figure 6b-c for illustration; Supplementary Table S7). Similarly, the total antioxidant
400 capacity (TAC) increased linearly with temperature (Linear regression, *p<0.05*; Figure 7, Supplementary
401 Table S8). However, the model explained only a weak part of the variation (R^2=0.1).

402

403 **4. Discussion**

404 4.1 Effects of temperature on coral metabolism

405 In the present study, the absolute value of oxygen consumption (most values between 0.05 and 0.1
406 µmol O_2 h^{-1} cm^{-2}) is hardly comparable with other values obtained previously in the literature due to
407 the paucity of research on antipatharian physiology and difference in the normalization method used
408 (Rakka et al., 2020). Studies conducted on scleractinian corals from the euphotic zone generally
409 reported much higher dark oxygen consumption rates (around 0.1-0.6 µmol h^{-1} cm^{-2} for tropical
410 scleractinians, Jurriaans & Hoogenboom, 2020; and most values between 0.1 and 1 µmol h^{-1} cm^{-2} for
411 temperate scleractinians, Aichelman et al., 2019). Such discrepancy may occur for several reasons.
412 Lower oxygen consumption rates have previously been observed at mesophotic depths as compared
413 to shallow waters, with *e.g.* 58 and 22% lower rates at 60 m compared to the surface in two species of
414 scleractinian corals (Cooper et al., 2011). Other studies suggested that metabolic demand reduction
415 through decreased respiration, growth or calcification rate may represent an adaptation to lowered
416 light levels at depths (Anthony & Hoegh-Guldberg, 2003; Cooper et al., 2011; Grigg, 2006; Huston,
417 1985, Eyal et al. 2019). In all cases, this was linked to the number, metabolism or clade of *Symbiodinium*
418 associated with the scleractinian. In most antipatharians, *Symbiodiniaceae* symbionts occur at very low
419 density and the lack or low density of *Symbiodiniaceae* in antipatharians might account, at least for a

part of their low respiration rate compared to euphotic scleractinians. This hypothesis is supported by respiration rates of ca. 0.08 and 0.2 µmoles O_2 h^{-1} cm^{-2} measured in deep cold-water scleractinians (218-690 m) with no *Symbiodiniaceae*, albeit at a much lower temperature (Naumann et al 2014). The large size and low density of the polyps (6.3 ± 0.07 polyps cm^{-2}, mean ± se, n=98) due to their localization on solely one row along the colony as compared to scleractinian corals (*e.g.* 112 polyps cm^{-2} in *Acropora hyacinthus*; 33 polyps cm^{-2} in *Pocillopora damicornis*; Coral Trait Database, 2021) may also be responsible for the lower oxygen consumption rates. Indeed, scleractinians with large polyps respire less by unit surface area than corals with smaller polyps, as the surface area to volume ratio is smaller, which slows down metabolic exchange rates (Anthony & Hoegh-Guldberg, 2003; Falkowski et al., 1990; Kahng et al., 2010; Kahng et al., 2019; Rossi et al., 2018).

The metabolic rates of *Stichopathes sp.* in our study were always outside the typical range of two to threefold linear increase for a 10°C increase (*i.e.* all Q_{10} values were outside 2-3), which suggests that the respiration rates did not follow the typical temperature-dependent reactions, and that additional processes requiring respiration were involved (Dodds et al., 2007). The wide range of Q_{10} values (from 0.68 to 47.05) suggests that the species has distinct metabolic performances at different temperatures (Previati et al., 2010). These differences are likely related to the duration of exposure as Q_{10} values tended to increase (Q_{10} 47.05 between 26-27.5°C) or decrease (Q_{10} 0.68 between 27.5-29°C) after 16 days. Previous studies showed that Q_{10} may tend to decrease with time of adjustment and tend to one when perfectly acclimatized (Barnes et al., 2001; Maier et al., 2013). We suggest that the sharp decrease in Q_{10} between 27.5 and 29°C resulted from the detrimental effects of temperature extremes on the condition of *Stichopathes sp.* (as in Dodds et al., 2007).

This hypothesis is further supported by the results obtained for healing capacity and tissue necrosis, which are interrelated processes as the capacity to heal directly impacts the ability of the coral to counter tissue necrosis. Indeed, while the healing rate (β) was significantly faster at 27.5°C than in the control, it was not the case at 29°C, which is beyond T_{opt} for respiration (28.3°C). In parallel, tissue

445 necrosis significantly increased at 29°C. The latter can be due to cell death and/or to the release of
446 free-living and mobile propagules from the coral polyps. Such process of asexual reproduction, called
447 polyp bail-out, was described recently on *Antipathella subpinnata* submitted to stressful conditions
448 (Coppari et al., 2020) and we also witnessed this process in *Stichopathes sp.* during new heat-stress
449 experiments (Godefroid, unpubl. obs.).

450 In contrast with the aforementioned parameters, the density of mucocytes in the tentacle epidermis
451 and TAC levels did not show any tipping point but increased linearly with temperature. Mucocyte
452 density is not a direct measure of mucus production but is very probably related to the latter, which is
453 further supported by the enlarged aspect of the cells, strongly suggesting an increased mucocyte
454 activity. The absence of tipping point in both mucocyte activity and TAC levels, which are widely used
455 as indicators of stress levels, likely reflects that both processes are still being used by the coral to
456 counter the effects of increasing temperatures, even past T_{opt} for respiration. Mucus production may
457 be used as a defence against biofouling, pathogens, pollution, UV radiation, sedimentation or
458 desiccation under stressful conditions (Brown & Bythell, 2005; Dellisanti et al., 2020; Ritchie, 2006;
459 Wild et al., 2004). Moreover, its adhesive properties act as a particle trap, critical for coral feeding
460 (Hadaidi et al., 2019), so the increase of food capture through the enhancement of mucus production
461 may serve as a helpful strategy when *Stichopathes sp.* is energetically impaired (Fransolet et al., 2013).
462 Finally, mucus may serve as a defence against pathogens when other immune defence mechanisms
463 are altered by thermal stress (Palmer et al., 2010; Wright et al., 2019). Oxidative stress parameters,
464 such as the endogenous levels of antioxidants, were suggested as effective biomarkers of stress for
465 multiple marine organisms, including corals (De Freitas Prazeres et al., 2012; Downs et al., 2005; 2011;
466 2012; Luz et al., 2018; Marangoni et al., 2017; Stuhr et al., 2017). Here, the increased TAC levels
467 indicate that the corals are investing in antioxidant defences, a compensatory response to increasing
468 thermal stress (Da Silva Fonseca et al., 2021; Marangoni et al., 2019; Marques et al., 2020). The steady
469 increase likely reflects that the antioxidant capacity of the corals has not yet reached a tipping point,
470 being overwhelmed by oxidative stress. Regardless of their functions, the increase of both parameters

with temperature concurs with the other endpoints in showing that *Stichopathes sp.* experienced temperature-related stress during the experiment.

Finally, no trends were observed for ammonium excretion and O:N ratio according to temperature. Ammonium excretion rate is often measured in conjunction with oxygen consumption rate to comprehensively describe the energetics of an organism under stressful conditions. Ammonium excretion rates are rarely measured in scleractinian corals as they usually have zooxanthellae that recycle the ammonium as part of the holobiont machinery, preventing measurements as ammonium concentrations are too low (Szmant et al., 1990). However, ammonium excretion has been shown to increase with temperature in azooxanthellate corals such as the cold-water scleractinian *Lophelia pertusa* (Dorey et al., 2020). While we expected similar results, the high variability in the data prevented us from drawing any trend. Often, the ammonium concentration was higher in control chambers than in chambers with nubbins. We suggest that this may result from the activity of the antipatharian holobiont, with associated microorganisms recycling the nitrogen produced by the host and present in the filtered seawater. These recycling organisms are unlikely to be *Symbiodiniaceae* as our fragments seemed to be azooxanthellate (based on histological and metabarcoding analyses, data not shown). Several studies revealed the high diversity (Liu et al., 2018; Santiago-Vázquez et al., 2007) and plasticity (van de Water et al., 2020) in microbial communities associated with antipatharian corals, which role in nitrogen cycling within the holobiont has been demonstrated previously in scleractinians (Middelburg et al., 2016; Szmant et al., 1990; see Rädecker et al., 2015 for review). Here, microbial diversity was not investigated genetically, but histological analyses revealed the presence of cell-associated microbial aggregates (CAMAs) in the ectoderm of the tentacles (Figure 6b). CAMAs were previously found in tissues of healthy scleractinians (Wada et al., 2019; Work & Aeby, 2014) and sea anemones (Palincsar et al., 1989), but it is described for the first time in antipatharians. This deserves further studies as scleractinian holobiont community was shown to shift in response to environmental stressors (Glasl et al., 2016; Kelly et al., 2014), including increasing temperature (Bourne

et al., 2008; Littman et al., 2011; Shiu et al., 2017; Thurber et al., 2009) and is likely to play a role in the resilience of antipatharians to future oceanic changes.

Similarly, no trend was observed in O:N ratio according to temperature. This ratio allows to detect a potential shift in the metabolic substrate used for catabolism (Mayzaud & Conover, 1988), indicating metabolic stress (Zhonge et al., 2013). This was observed with the gorgonian coral *Primnora researeformis* (Scanes et al., 2018) but other studies showed no effect of temperature on O:N ratio in cold-water corals (*Desmophyllum dianthus*, Gori et al., 2016). Here, we expected to see a shift as most parameters showed to be impacted by temperature, but results are difficult to interpret as the impact of nitrogen-cycling bacteria on these measured excretion rates is unknown, leading to high variability in the ammonium excretion rates measurements.

4.2 Ecological implications

Considering that a biological response to any environmental driver is curvilinear, any variation around a sub or supra optimal mean value should lower the performance of an organism (Ruel et al., 1999; Pansch & Hiebenthal, 2019). Part of our results are in line with this theoretical perspective, with the metabolic rate of *Stichopathes sp.* revealing a bell-shaped curve with an intermediate optimum around 28.3°C. Apart from this tipping point, performances start to decrease through lower oxygen consumption rates.

The present results revealed that there is an important mismatch between the thermal optimum (T_{opt}) of *Stichopathes sp.* at the end of the coldest months of the year (October-November) and the mean environmental temperature at the same period. Indeed, T_{opt} (28.3°C) was 2.7°C above the mean environmental temperature (25.6°C), suggesting that *Stichopathes sp.* functions at suboptimal performances during the coldest months of the year. Even when temperature fluctuations attributed to internal waves are considered, T_{opt} remains 0.6°C above the maximum temperature of the environment (27.7°C, Figure 2e). Moreover, given that T_{opt} did not align to the mean environmental

temperature, despite the fact that it is the end of the cold season and *Stichopathes sp.* had several months to acclimatize to these conditions, this suggests that *Stichopathes sp.* has poor thermal acclimatization capacity and/or that its rate of acclimatization is too low on the seasonal scale (Jurriaans & Hoogenboom, 2019). *Stichopathes sp*. might also live at temperatures lower than T_{opt} because the thermal environmental fluctuations (*i.e.* the internal waves) are unpredictable, making acclimatization across seasons ineffective (Gabriel, 2005; Gilchrist, 1995; Jurriaans & Hoogenboom, 2020). On the contrary, during the warm season, T_{opt} will be very close to the mean environmental temperature (28.3°C at 50 m), resulting in better performance at that period. However, this also means that the risk of exceeding T_{opt} during the warm season is high, except if *Stichopathes sp.* shows warm acclimatization abilities. This could be tested by running a similar experiment during the summer months (April).

Increased temperatures elicited other stress responses: impairment of the healing capacity (from +4.5°C, 30.5°C) and increased tissue necrosis (from +3°C, 29°C). Mucocyte activity and antioxidants production showed a linear increase with temperature (see Figure 8 for a summary of the results). The difference in temperature between T_{opt} (28.3°C) and these first signs of stress (around 29°C) is small, suggesting a narrow thermal window of performance (T_{br}) for *Stichopathes sp.* A small thermal performance breadth reflects a sharp peaked thermal sensitivity, which translates into high susceptibility to increasing temperatures (as, for instance, in *Acropora valenciennesi*, Jurriaans & Hoogenboom, 2020).

Altogether, the poor/slow acclimatization capacity and narrow thermal breadth of *Stichopathes sp.* suggest that it is likely to be affected by increasing temperatures, if the effects observed in aquarium also apply in the natural environment. This does not support the idea that temperature fluctuations associated with internal waves create thermal refugia in which heat stress may be buffered (Reardon et al., 2018; Wall et al., 2015; Wyatt et al., 2020). Similarly, a study in the Caribbean showed that

thermal internal waves did not allow mesophotic scleractinians to acclimatize to heat stress. Actually, the latter had lower bleaching thresholds than shallow water corals (Smith et al., 2016).

While it is clear that mean maximum temperatures will increase at mesophotic depths based on emission scenarios, models forecasting changes in environmental variability are few (Bates et al., 2018). Recent models, developed to predict thermal stress through the mesophotic zone, highlighted that heat stress exposure will not decrease with depth and that MCEs may not be refugia (Schramek et al., 2018; Venegas et al., 2019). Very roughly, we extrapolated our results by simulating an increase by 1°C from the temperatures measured in Oct-Nov (Figure 9). Even with this extra 1°C, the mean environmental temperature would remain 1.7°C below T_{opt}. However, T_{opt} could be exceeded if considering the internal waves, which may then impact the metabolism of *Stichopathes sp*. if it has not acclimatized to these new environmental conditions (*i.e.* if T_{opt} remains constant). Acclimatization at longer term than the present experiment (16 days) cannot be ruled out. However, the present experiment has the same time scale than internal waves, meaning that acclimatization, if any, could already have occurred. Finally, considering the long life span of antipatharian colonies (varying among species on the order of decades to millennia; Wagner et al., 2012), adaptation is probably not to be expected at the time scale of ocean warming. As *Stichopathes sp.* does not rely on light, it could escape to deeper and colder waters providing these are rich enough in food.

5. Conclusion

The optimal temperature for respiration (around 28.3°C), calculated during the coldest months of the year for the mesophotic antipatharian *Stichopathes sp.*, was well above the mean local environmental temperature, suggesting that *Stichopathes sp.* has poor acclimatization capacity and/or that its acclimatization rate is too low for the seasonal scale. However, its performances started to decrease beyond T_{opt}, with reduced oxygen consumption rate, impairment of the healing capacities and higher tissue necrosis. Furthermore, mucocyte density and TAC production increased linearly with

temperature, as often observed for typical stress responses, inducing further energetic costs. Based on these additive and complementary observations, we suggest that *Stichopathes sp.* has a narrow thermal breadth and that the exceedance of T_{opt} would have significant consequences for this species. This could occur during the warm season when the mean environmental temperature is very close to T_{opt} but also during the cold season with only 1°C increase.

Acknowledgments

M. Godefroid is holder of a Belgian FRIA grant. Ph. Dubois is a Research Director of the National Fund for Scientific Research (FRS-FNRS; Belgium). L. Hédouin is a CNRS Research Fellow (France). We would like to thank Y. Lacube for his advices with the maintenance of the aquaria, B. Espiau for teaching the alkalinity anomaly technique, L. Terrana for his expertise regarding the taxonomy of antipatharians and the histological protocol used, Ph. Pernet for the histological training. We thank I. Eeckhout for the access to the ZEISS microscope and associated camera and V. Parravicini for the use of his respirometry equipment. Service National d'Observation (SNO) CORAIL from CRIOBE kindly provided data. Under The Pole Consortium: G. Bardout, A. Ferucci, F. Gazzola, G. Lagarrigue, J. Leblond, E. Marivint, N. Mollon, N. Paulme, E. Périé-Bardout, S. Pujolle, G. Siu.

Funding sources

This work was supported by the King Leopold III Fund for Nature Exploration and Conservation and by the FNRS project COBICO (Grant number T0084.18).

Credit author statement

Mathilde Godefroid: Conceptualization, Methodology, Formal analysis, Investigation, Writing – Original Draft, Visualisation; Laetitia Hédouin: Conceptualization, Methodology, Resources, Writing – Review & Editing; Alexandre Mercière: Software, Resources; Under The Pole Consortium: Resources; Philippe Dubois: Conceptualization, Methodology, Resources, Writing – Review & Editing.

Literature cited

Aichelman, H.E., Zimmerman, R.C., & Barshis, D.J. (2019). Adaptive signatures in thermal performance of the temperate coral *Astrangia poculata*. *The Journal of Experimental Biology*, *222*(5), jeb189225.

Angilletta, M.J. (2009). *Thermal adaptation: A theoretical and empirical synthesis*. Oxford University Press.

Anthony, K.R.N., & Hoegh-Guldberg, O. (2003). Variation in coral photosynthesis, respiration and growth characteristics in contrasting light microhabitats: An analogue to plants in forest gaps and understoreys? *Functional Ecology*, *17*(2), 246–259.

Antonius, A., & Ballesteros, E. (1998). Epizoism: A new threat to coral health in Caribbean reefs. *Revista de biologia tropical,* 12.

Barnes, R.S.K., Calow, P., Olive, P.J.W., Golding, D.W., & Spicer, J.I. (2001). The Invertebrates–A Synthesis. 505 pp.

Bates, A.E., Helmuth, B., Burrows, M.T., Duncan, M.I., Garrabou, J., Guy-Haim, T., et al. (2018). Biologists ignore ocean weather at their peril. *Nature*, 299-301.

Battisti, C., Poeta, G., & Fanelli, G. (2016). An introduction to disturbance ecology. *Cham: Springer*, 13-29.

Bo, M., Baker, A., Gaino, E., Wirshing, H., Scoccia, F., & Bavestrello, G. (2011). First description of algal mutualistic endosymbiosis in a black coral (Anthozoa: Antipatharia). *Marine Ecology Progress Series*, *435*, 1–11.

Bo, M., Bavestrello, G., Di Muzio, G., Canese, S., & Betti, F. (2019). First record of a symbiotic relationship between a polyclad and a black coral with description of *Anthoplana antipathellae* gen. Et sp. Nov. (Acotylea, Notoplanidae). *Marine Biodiversity*, *49*(6), 2549-2570.

620 Bo, M., Canese, S., & Bavestrello, G. (2014). Discovering Mediterranean black coral forests:
621 *Parantipathes larix* (Anthozoa: Hexacorallia) in the Tuscan Archipelago, Italy. *Italian Journal of*
622 *Zoology*, *81*(1), 112–125.
623 Bo, M., Montgomery, A.D., Opresko, D.M., Wagner, D., & Bavestrello, G. (2019). Antipatharians of the
624 mesophotic zone: four case studies. In Y. Loya, K.A. Puglise, & T.C.L. Bridge (Eds.), *Mesophotic*
625 *Coral Ecosystems* (Vol. 12, pp. 683–708). Springer International Publishing.
626 Bo, M., Tazioli, S., Spanò, N., & Bavestrello, G. (2008). *Antipathella subpinnata* (Antipatharia,
627 Myriopathidae) in Italian seas. *Italian Journal of Zoology*, *75*(2), 185–195.
628 Bongaerts, P., Ridgway, T., Sampayo, E.M., & Hoegh-Guldberg, O. (2010). Assessing the 'deep reef
629 refugia' hypothesis: focus on Caribbean reefs. *Coral Reefs*, *29*(2), 309–327.
630 Bongaerts, P., Riginos, C., Brunner, R., Englebert, N., Smith, S.R., & Hoegh-Guldberg, O. (2017). Deep
631 reefs are not universal refuges: reseeding potential varies among coral species. *Science*
632 *Advances*, 3(2), e1602373.
633 Bongaerts, P., & Smith, T.B. (2019). Beyond the "Deep Reef Refuge" hypothesis: a conceptual
634 framework to characterize persistence at depth. In Y. Loya, K.A. Puglise, & T.C.L. Bridge (Eds.),
635 *Mesophotic Coral Ecosystems* (Vol. 12, pp. 881–895). Springer International Publishing.
636 Bosch, T.C.G., & McFall-Ngai, M.J. (2011). Metaorganisms as the new frontier. *Zoology*, *114*(4), 185–
637 190.
638 Bourne, D., Iida, Y., Uthicke, S., & Smith-Keune, C. (2008). Changes in coral-associated microbial
639 communities during a bleaching event. *The ISME Journal*, *2*(4), 350–363.
640 Bridge, T.C., Hoey, A.S., Campbell, S.J., Muttaqin, E., Rudi, E., Fadli, N., & Baird, A.H. (2013). Depth-
641 dependent mortality of reef corals following a severe bleaching event: implications for thermal
642 refuges and population recovery. *F1000Research*, *2*.
643 Brown, B., & Bythell, J. (2005). Perspectives on mucus secretion in reef corals. *Marine Ecology Progress*
644 *Series*, *296*, 291–309.

Bruckner, A., Angelis, P.D., & Montgomery, T. (2008). Case study for black coral from Hawaii. In *International Expert Workshop on CITES Non-detriment Findings, Cancun, November 17th–22nd*.

Bruckner, A.W. (2016). Advances in management of precious corals to address unsustainable and destructive harvest techniques. In S. Goffredo & Z. Dubinsky (Eds.), *The Cnidaria, Past, Present and Future* (pp. 747–786). Springer International Publishing.

Cairns, S.D. (2007). Deep-water corals: an overview with special reference to diversity and distribution of deep-water scleractinian corals. *Bulletin of marine science*, *81*(3), 12.

Cooper, T.F., Ulstrup, K.E., Dandan, S.S., Heyward, A.J., Kühl, M., Muirhead, A., O'Leary, R.A., Ziersen, B.E.F., & Van Oppen, M.J.H. (2011). Niche specialization of reef-building corals in the mesophotic zone: Metabolic trade-offs between divergent *Symbiodinium* types. *Proceedings of the Royal Society B: Biological Sciences*, *278*(1713), 1840–1850.

Coppari, M., Fumarola, L., Bramanti, L., Romans, P., Pillot, R., Bavestrello, G., & Bo, M. (2020). Unveiling asexual reproductive traits in black corals: Polyp bail-out in *Antipathella subpinnata*. *Coral Reefs*, *39*(6), 1517-1523.

Dannenberg, R.P. (2015). Characterization and Oil Response of the Deep Sea Coral-associated Microbiome.

da Silva Fonseca, J., Mies, M., Paranhos, A., Taniguchi, S., Güth, A.Z., Bícego, M.C., Marques, J.A., Fernandes de Barros Marangoni, L., & Bianchini, A. (2021). Isolated and combined effects of thermal stress and copper exposure on the trophic behavior and oxidative status of the reef-building coral *Mussismilia harttii. Environmental Pollution*, *268*, 115892.

De Assis, J., Souza, J., Lima, M., Lima, G., Cordeiro, R., & Pérez, C. (2019). Association between deep-water scale-worms (Annelida: Polynoidae) and black corals (Cnidaria: Antipatharia) in the Southwestern Atlantic. *Zoologia*, *36*, 1–13.

669 De Clippele, L.H., Huvenne, V.A.I., Molodtsova, T.N., & Roberts, J.M. (2019). The diversity and
670 ecological role of non-scleractinian corals (Antipatharia and Alcyonacea) on scleractinian cold-
671 water coral mounds. *Frontiers in Marine Science*, *6*, 184.
672 de Freitas Prazeres, M., Martins, S.E., & Bianchini, A. (2012). Assessment of water quality in coastal
673 waters of Ferando de noronha, Brazil: Biomarker analyses in *Amphistegina lessonii. The Journal*
674 *of Foraminiferal Research*, *42*(1), 56–65.
675 Dell, A.I., Pawar, S., & Savage, V.M. (2011). Systematic variation in the temperature dependence of
676 physiological and ecological traits. *Proceedings of the National Academy of Sciences*, *108*(26),
677 10591–10596.
678 Dell, A.I., Pawar, S., & Savage, V.M. (2013). The thermal dependence of biological traits: Ecological
679 Archives. *Ecology*, *94*(5), 1205–1206.
680 Dellisanti, W., Tsang, R.H.L., Ang, P., Wu, J., Wells, M.L., & Chan, L.L. (2020). Metabolic performance
681 and thermal and salinity tolerance of the coral *Platygyra carnosa* in Hong Kong waters. *Marine*
682 *Pollution Bulletin*, *153*, 111005.
683 Deutsch, C.A., Tewksbury, J.J., Huey, R.B., Sheldon, K.S., Ghalambor, C.K., Haak, D.C., & Martin, P.R.
684 (2008). Impacts of climate warming on terrestrial ectotherms across latitude. *Proceedings of*
685 *the National Academy of Sciences*, *105*(18), 6668–6672.
686 Dorey, N., Gjelsvik, Ø., Kutti, T., & Büscher, J.V. (2020). Broad thermal tolerance in the cold-water coral
687 *Lophelia pertusa* from Arctic and Boreal reefs. *Frontiers in Physiology*, *10*, 1636.
688 Downs, C.A., Fauth, J.E., Robinson, C.E., Curry, R., Lanzendorf, B., Halas, J.C., Halas, J., & Woodley, C.M.
689 (2005). Cellular diagnostics and coral health: Declining coral health in the Florida Keys. *Marine*
690 *Pollution Bulletin*, *51*(5–7), 558–569.
691 Downs, C.A., Ostrander, G.K., Rougee, L., Rongo, T., Knutson, S., Williams, D.E., Mendiola, W.,
692 Holbrook, J., & Richmond, R.H. (2012). The use of cellular diagnostics for identifying sub-lethal
693 stress in reef corals. *Ecotoxicology*, *21*(3), 768–782.

694 Downs, C.A., Woodley, C.M., Fauth, J.E., Knutson, S., Burtscher, M.M., May, L.A., Avadanei, A.R.,
695 Higgins, J.L., & Ostrander, G.K. (2011). A survey of environmental pollutants and cellular-stress
696 markers of *Porites astreoides* at six sites in St. John, U.S. Virgin Islands. *Ecotoxicology*, *20*(8),
697 1914–1931.
698 Falkowski, P.G., Jokiel, P.L., & Kinzie, R.A. (1990). Irradiance and corals. *Ecosystems of the world*, *25*,
699 89-107.
700 Forstner, H. (1983). An Automated Multiple-Chamber Intermittent-Flow Respirometer. In
701 *Polarographic Oxygen Sensors* (Polarographic Oxygen Sensors, pp. 111–126). Springer.
702 Frade, P.R., Bongaerts, P., Englebert, N., Rogers, A., Gonzalez-Rivero, M., & Hoegh-Guldberg, O. (2018).
703 Deep reefs of the Great Barrier Reef offer limited thermal refuge during mass coral bleaching.
704 *Nature Communications*, *9*(1), 1-8.
705 Fransolet, D., Roberty, S., Herman, A.C., Tonk, L., Hoegh-Guldberg, O., & Plumier, J.C. (2013). Increased
706 cell proliferation and mucocyte density in the sea anemone *Aiptasia pallida* recovering from
707 bleaching. *PLoS ONE*, *8*(5), e65015.
708 Frazier, M.R., Huey, R.B., & Berrigan, D. (2006). Thermodynamics constrains the evolution of insect
709 population growth rates: "Warmer Is Better". *The American Naturalist*, *168*(4), 512–520.
710 Gabriel, W. (2005). How stress selects for reversible phenotypic plasticity. *Journal of Evolutionary*
711 *Biology*, *18*(4), 873–883.
712 Gilchrist, G.W. (1995). Specialists and generalists in changing environments. I. Fitness landscapes of
713 thermal sensitivity. *The American Naturalist*, *146*(2), 252–270.
714 Glasl, B., Herndl, G.J., & Frade, P.R. (2016). The microbiome of coral surface mucus has a key role in
715 mediating holobiont health and survival upon disturbance. *The ISME Journal*, *10*(9), 2280–
716 2292.
717 Glynn, P.W. (1996). Coral reef bleaching: Facts, hypotheses and implications. *Global Change Biology*,
718 *2*(6), 495–509.

719 Goldberg, W.M. (1978). Chemical changes accompanying maturation of the connective tissue
720 skeletons of gorgonian and antipatharian corals. *Marine Biology*, *49*(3), 203–210.
721 Goldberg, W.M., Hopkins, T.L., Holl, S.M., Schaefer, J., Kramer, K.J., Morgan, T.D., & Kim, K. (1994).
722 Chemical composition of the sclerotized black coral skeleton (Coelenterata: Antipatharia): a
723 comparison of two species. *Comparative Biochemistry and Physiology Part B: Comparative*
724 *Biochemistry*, *107*(4), 633-643.
725 Gori, A., Ferrier-Pagès, C., Hennige, S.J., Murray, F., Rottier, C., Wicks, L.C., & Roberts, J.M. (2016).
726 Physiological response of the cold-water coral *Desmophyllum dianthus* to thermal stress and
727 ocean acidification. *PeerJ*, *4*, e1606.
728 Gress, E., Eeckhaut, I., Godefroid, M., Dubois, P., Richir, J., & Terrana, L. (2021). Investigating densities
729 of Symbiodiniaceae in two species of Antipatharians (black corals) from Madagascar. *bioRxiv.*
730 Grigg, R.W. (2001). Black Coral: History of a sustainable fishery in Hawai'i. *Pacific Science*, *55*(3), 291–
731 299.
732 Grigg, R.W. (2006). Depth limit for reef building corals in the Au'au Channel, S.E. Hawaii. *Coral Reefs*,
733 *25*(1), 77–84.
734 Hadaidi, G., Gegner, H.M., Ziegler, M., & Voolstra, C.R. (2019). Carbohydrate composition of mucus
735 from scleractinian corals from the central Red Sea. *Coral Reefs*, *38*(1), 21–27.
736 Holling, C.S. (1973). Resilience and Stability of Ecological Systems. *Annual Review of Ecology and*
737 *Systematics*, *4*(1), 1–23.
738 Huang, D., Ou, B., & Prior, R.L. (2005). The chemistry behind antioxidant capacity assays. *Journal of*
739 *agricultural and food chemistry*, *53*(6), 1841-1856.
740 Huey, R., & Stevenson, R. (1979). Integrating thermal physiology and ecology of ectotherms: A
741 discussion of approaches. *American Zoologist*, *19*(1), 357–366.
742 Hughes, D.J., & Narayanaswamy, B.E. (2013). Impacts of climate change on deep-sea habitats. *MCCIP*
743 *Science Review 2013*, 7 pages.

744 Hughes, T.P., Kerry, J.T., Álvarez-Noriega, M., Álvarez-Romero, J.G., Anderson, K.D., Baird, A.H.,
745 Babcock, R.C., Beger, M., Bellwood, D.R., Berkelmans, R., Bridge, T.C., Butler, I.R., Byrne, M.,
746 Cantin, N.E., Comeau, S., Connolly, S.R., Cumming, G.S., Dalton, S.J., Diaz-Pulido, G., … Wilson,
747 S. K. (2017). Global warming and recurrent mass bleaching of corals. *Nature*, *543*(7645), 373–
748 377.
749 Huston, M. (1985). Variation in coral growth rates with depth at Discovery Bay, Jamaica. *Coral Reefs*,
750 *4*(1), 19–25.
751 IPCC. (2018). Summary for Policymakers. In: *Global Warming of 1.5°C. An IPCC Special Report on the*
752 *impacts of global warming of 1.5°C above pre-industrial levels and related global greenhouse*
753 *gas emission pathways, in the context of strengthening the global response to the threat of*
754 *climate change, sustainable development, and efforts to eradicate poverty* [Masson-Delmotte,
755 V., P. Zhai, H.O. Pörtner, D. Roberts, J. Skea, P.R. Shukla, A. Pirani, W. Moufouma-Okia, C. Péan,
756 R. Pidcock, S. Connors, J.B.R. Matthews, Y. Chen, X. Zhou, M.I. Gomis, E. Lonnoy, T. Maycock,
757 M. Tignor, and T. Waterfield (eds.)]. *World Meteorological Organization, Geneva, Switzerland,*
758 *32 pp.*

759 IPCC. (2019). Summary for Policymakers. In: IPCC Special Report on the Ocean and Cryosphere in a
760 Changing Climate [H.O. Pörtner, D.C. Roberts, V. Masson-Delmotte, P. Zhai, M. Tignor, E.
761 Poloczanska, K. Mintenbeck, A. Alegría, M. Nicolai, A. Okem, J. Petzold, B. Rama, N.M. Weyer
762 (eds.)]. In press.

763 Juárez-de la Rosa, B.A., Muñoz-Saldaña, J., Torres-Torres, D., Ardisson, P.L., & Alvarado-Gil, J.J. (2012).
764 Nanoindentation characterization of the micro-lamellar arrangement of black coral skeleton.
765 *Journal of Structural Biology*, *177*(2), 349–357.
766 Jurriaans, S., & Hoogenboom, M. (2020). Seasonal acclimation of thermal performance in two species
767 of reef-building corals. *Marine Ecology Progress Series*, *635*, 55–70.

768 Jurriaans, S., & Hoogenboom, M.O. (2019). Thermal performance of scleractinian corals along a
769 latitudinal gradient on the Great Barrier Reef. *Philosophical Transactions of the Royal Society*
770 *B, 374*(1778), 20180546.
771 Kahng, S.E., Akkaynak, D., Shlesinger, T., Hochberg, E.J., Wiedenmann, J., Tamir, R., & Tchernov, D.
772 (2019). Light, temperature, photosynthesis, heterotrophy, and the lower depth limits of
773 Mesophotic Coral Ecosystems. In Y. Loya, K. A. Puglise, & T. C. L. Bridge (Eds.), *Mesophotic Coral*
774 *Ecosystems* (Vol. 12, pp. 801–828). Springer International Publishing.
775 Kahng, S.E., Garcia-Sais, J.R., Spalding, H.L., Brokovich, E., Wagner, D., Weil, E., Hinderstein, L., &
776 Toonen, R.J. (2010). Community ecology of mesophotic coral reef ecosystems. *Coral Reefs*,
777 *29*(2), 255–275.
778 Kelly, L.W., Williams, G.J., Barott, K.L., Carlson, C.A., Dinsdale, E.A., Edwards, R.A., Haas, A.F., Haynes,
779 M., Lim, Y.W., McDole, T., Nelson, C.E., Sala, E., Sandin, S.A., Smith, J.E., Vermeij, M.J.A., Youle,
780 M., & Rohwer, F. (2014). Local genomic adaptation of coral reef-associated microbiomes to
781 gradients of natural variability and anthropogenic stressors. *Proceedings of the National*
782 *Academy of Sciences*, *111*(28), 10227–10232.
783 Kim, K., Goldberg, W.M., & Taylor, G.T. (1992). Architectural and mechanical properties of the black
784 coral skeleton (Coelenterata: Antipatharia): a comparison of two species. *The Biological*
785 *Bulletin*, *182*(2), 195–209.
786 Leichter, J.J., Helmuth, B., & Fischer, A.M. (2006). Variation beneath the surface: Quantifying complex
787 thermal environments on coral reefs in the Caribbean, Bahamas and Florida. *Journal of Marine*
788 *Research*, *64*(4), 563–588.
789 Levin, L.A., & Le Bris, N. (2015). The deep ocean under climate change. *Science*, *350*(6262), 766–768.
790 Lindfield, S.J., Harvey, E.S., Halford, A.R., and McIlwain, J.L. (2016). Mesophotic depths as refuge areas
791 for fishery-targeted species on coral reefs. *Coral Reefs*, *35*(1), 125–137.

792 Littman, R., Willis, B.L., & Bourne, D.G. (2011). Metagenomic analysis of the coral holobiont during a
793 natural bleaching event on the Great Barrier Reef: Metagenomics analysis of bleached coral.
794 *Environmental Microbiology Reports*, *3*(6), 651–660.
795 Liu, Y.C., Huang, R.M., Bao, J., Wu, K.Y., Wu, H.Y., Gao, X.Y., & Zhang, X.Y. (2018). The unexpected
796 diversity of microbial communities associated with black corals revealed by high-throughput
797 Illumina sequencing. *FEMS Microbiology Letters*, *365*(15).
798 Logan, C.A., Dunne, J.P., Eakin, C.M., & Donner, S.D. (2014). Incorporating adaptive responses into
799 future projections of coral bleaching. *Global Change Biology*, *20*(1), 125–139.
800 Luz, D.C., Zebral, Y.D., Klein, R.D., Marques, J.A., Marangoni, L.F. de B., Pereira, C.M., Duarte, G.A.S.,
801 Pires, D.O., Castro, C.B., Calderon, E.N., & Bianchini, A. (2018). Oxidative stress in the
802 hydrocoral *Millepora alcicornis* exposed to CO2-driven seawater acidification. *Coral Reefs*,
803 *37*(2), 571–579.
804 Maier, C., Bils, F., Weinbauer, M.G., Watremez, P., Peck, M.A., & Gattuso, J.P. (2013). Respiration of
805 Mediterranean cold-water corals is not affected by ocean acidification as projected for the end
806 of the century. *Biogeosciences*, *10*(8), 5671–5680.
807 Marangoni, L.F.B., Dalmolin, C., Marques, J.A., Klein, R.D., Abrantes, D.P., Pereira, C.M., Calderon, E.N.,
808 Castro, C.B., & Bianchini, A. (2019). Oxidative stress biomarkers as potential tools in reef
809 degradation monitoring: A study case in a South Atlantic reef under influence of the 2015–
810 2016 El Niño/Southern Oscillation (ENSO). *Ecological Indicators*, *106*, 105533.
811 Marangoni, L.F., Marques, J.A., Duarte, G.A.S., Pereira, C.M., Calderon, E.N., Castro, C.B., & Bianchini,
812 A. (2017). Copper effects on biomarkers associated with photosynthesis, oxidative status and
813 calcification in the Brazilian coral *Mussismilia harttii* (Scleractinia, Mussidae). *Marine*
814 *Environmental Research*, *130*, 248–257.
815 Marques, J.A., Flores, F., Patel, F., Bianchini, A., Uthicke, S., & Negri, A. P. (2020). Acclimation history
816 modulates effect size of calcareous algae (*Halimeda opuntia*) to herbicide exposure under
817 future climate scenarios. *Science of The Total Environment*, *739*, 140308.

818 Martin, T.L., & Huey, R.B. (2008). Why “suboptimal” is optimal: Jensen’s inequality and ectotherm
819 thermal preferences. *The American Naturalist*, *171*(3), e102–E118.
820 Mayzaud, P., & Conover, R. (1988). O:N atomic ratio as a tool to describe zooplankton metabolism.
821 *Marine Ecology Progress Series*, *45*, 289–302.
822 McFall-Ngai, M., Hadfield, M.G., Bosch, T.C.G., Carey, H.V., Domazet-Lošo, T., Douglas, A.E., Dubilier,
823 N., Eberl, G., Fukami, T., Gilbert, S.F., Hentschel, U., King, N., Kjelleberg, S., Knoll, A.H., Kremer,
824 N., Mazmanian, S.K., Metcalf, J.L., Nealson, K., Pierce, N.E., … Wernegreen, J.J. (2013). Animals
825 in a bacterial world, a new imperative for the life sciences. *Proceedings of the National*
826 *Academy of Sciences*, *110*(9), 3229–3236.
827 Middelburg, J.J., Mueller, C.E., Veuger, B., Larsson, A.I., Form, A., & Oevelen, D. (2016). Discovery of
828 symbiotic nitrogen fixation and chemoautotrophy in cold-water corals. *Scientific Reports*, *5*(1),
829 1-9.
830 Molodtsova, T. (2008). Anthozoa from the northern Mid-Atlantic Ridge and Charlie-Gibbs Fracture
831 Zone. *Marine Biology Research, 4*(1–2), 112–130.
832 Neal, B.P., Condit, C., Liu, G., dos Santos, S., Kahru, M., Mitchell, B.G., & Kline, D.I. (2014). When depth
833 is no refuge: Cumulative thermal stress increases with depth in Bocas del Toro, Panama. *Coral*
834 *Reefs*, *33*(1), 193–205.
835 Orejas, C., & Jiménez, C. (2017). The builders of the oceans – Part I: Coral architecture from the tropics
836 to the poles, from the shallow to the deep. In S. Rossi, L. Bramanti, A. Gori, & C. Orejas (Eds.),
837 *Marine Animal Forests* (pp. 1–30). Springer International Publishing.
838 Palincsar, E.E., Jones, W.R., Palincsar, J.S., Glogowski, M.A., & Mastro, J.L. (1989). Bacterial aggregates
839 within the epidermis of the sea anemone *Aiptasia pallida*. *The Biological Bulletin*, *177*(1), 130–
840 140.
841 Palmer, C.V., Bythell, J.C., & Willis, B.L. (2010). Levels of immunity parameters underpin bleaching and
842 disease susceptibility of reef corals. *The FASEB Journal*, *24*(6), 1935–1946.

Pansch, C., & Hiebenthal, C. (2019). A new mesocosm system to study the effects of environmental variability on marine species and communities. *Limnology and Oceanography: Methods*, *17*(2), 145–162.

Payne, N.L., Smith, J.A., Meulen, D.E., Taylor, M.D., Watanabe, Y.Y., Takahashi, A., Marzullo, T.A., Gray, C.A., Cadiou, G., & Suthers, I.M. (2016). Temperature dependence of fish performance in the wild: Links with species biogeography and physiological thermal tolerance. *Functional Ecology*, *30*(6), 903–912.

Penn, K., Wu, D., Eisen, J.A., & Ward, N. (2006). Characterization of bacterial communities associated with deep-sea corals on Gulf of Alaska seamounts. *Applied and Environmental Microbiology*, *72*(2), 1680–1683.

Portner, H.O. (2010). Oxygen- and capacity-limitation of thermal tolerance: A matrix for integrating climate-related stressor effects in marine ecosystems. *Journal of Experimental Biology*, *213*(6), 881–893.

Previati, M., Scinto, A., Cerrano, C., & Osinga, R. (2010). Oxygen consumption in Mediterranean octocorals under different temperatures. *Journal of Experimental Marine Biology and Ecology*, *390*(1), 39–48.

Pyle, R.L., Boland, R., Bolick, H., Bowen, B.W., Bradley, C.J., Kane, C., Kosaki, R.K., Langston, R., Longenecker, K., Montgomery, A., Parrish, F.A., Popp, B.N., Rooney, J., Smith, C.M., Wagner, D., & Spalding, H.L. (2016). A comprehensive investigation of mesophotic coral ecosystems in the Hawaiian Archipelago. *PeerJ*, *4*, e2475.

Rädecker, N., Pogoreutz, C., Voolstra, C.R., Wiedenmann, J., & Wild, C. (2015). Nitrogen cycling in corals: The key to understanding holobiont functioning? *Trends in Microbiology*, *23*(8), 490–497.

Rakka, M., Orejas, C., Maier, S.R., Van Oevelen, D., Godinho, A., Bilan, M., & Carreiro-Silva, M. (2020). Feeding biology of a habitat-forming antipatharian in the Azores Archipelago. *Coral Reefs*, *39*(5): 1469-1482.

869 Reardon, S. (2018). Hurricane Maria's wrath leaves clues to coral reefs' future. *Nature*, *560*(7719), 421-
870 423.

871 Ritchie, K. (2006). Regulation of microbial populations by coral surface mucus and mucus-associated
872 bacteria. *Marine Ecology Progress Series*, *322*, 1–14.

873 Rocha, L.A., Pinheiro, H.T., Shepherd, B., Papastamatiou, Y.P., Luiz, O.J., Pyle, R.L., & Bongaerts, P.
874 (2018). Mesophotic coral ecosystems are threatened and ecologically distinct from shallow
875 water reefs. *Science*, *361*(6399), 281–284.

876 Rodgers, G.G., Tenzing, P., & Clark, T.D. (2016). Experimental methods in aquatic respirometry: The
877 importance of mixing devices and accounting for background respiration: methods in aquatic
878 respirometry. *Journal of Fish Biology*, *88*(1), 65–80.

879 Rossi, S., Bramanti, L., Gori, A., & Orejas, C. (Eds.). (2017). *Marine Animal Forests: The Ecology of*
880 *Benthic Biodiversity Hotspots*. Springer International Publishing.

881 Rossi, S., Schubert, N., Brown, D., Soares, M., Grosso, V., Rangel-Huerta, E., & Maldonado, E. (2018).
882 Linking host morphology and symbiont performance in octocorals. *Scientific Reports*, *8*(1).

883 Ruel, J.J., & Ayres, M.P. (1999). Jensen's inequality predicts effects of environmental variation. *Trends*
884 *in Ecology & Evolution*, *14*(9), 361-366.

885 Santiago-Vázquez, L.Z., Brück, T.B., Brück, W.M., Duque-Alarcón, A.P., McCarthy, P.J., & Kerr, R.G.
886 (2007). The diversity of the bacterial communities associated with the azooxanthellate
887 hexacoral *Cirrhipathes lutkeni. The ISME Journal*, *1*(7), 654–659.

888 Scanes, E., Kutti, T., Fang, J.K.H., Johnston, E.L., Ross, P.M., & Bannister, R.J. (2018). Mine waste and
889 acute warming induce energetic stress in the deep-sea sponge *Geodia atlantica* and coral
890 *Primnoa resedeaformis*; results from a mesocosm study. *Frontiers in Marine Science*, *5*.

891 Schneider, C.A., Rasband, W.S., & Eliceiri, K.W. (2012). NIH Image to ImageJ: 25 years of image
892 analysis. *Nature methods, 9*(7): 671-675.

Schramek, T.A., Colin, P.L., Merrifield, M.A., & Terrill, E.J. (2018). Depth-dependent thermal stress around corals in the tropical Pacific ocean. *Geophysical Research Letters*, *45*(18), 9739–9747.

Schulte, P.M. (2015). The effects of temperature on aerobic metabolism: Towards a mechanistic understanding of the responses of ectotherms to a changing environment. *Journal of Experimental Biology*, *218*(12), 1856–1866.

Schulte, P.M., Healy, T.M., & Fangue, N.A. (2011). Thermal performance curves, phenotypic plasticity, and the time scales of temperature exposure. *Integrative and Comparative Biology*, *51*(5), 691–702.

Shiu, J.H., Keshavmurthy, S., Chiang, P.W., Chen, H.J., Lou, S.P., Tseng, C.H., Justin Hsieh, H., Allen Chen, C., & Tang, S.L. (2017). Dynamics of coral-associated bacterial communities acclimated to temperature stress based on recent thermal history. *Scientific Reports*, *7*(1).

Smith, T.B., Brandtneris, V.W., Canals, M., Brandt, M.E., Martens, J., Brewer, R.S., Kadison, E., Kammann, M., Keller, J., & Holstein, D.M. (2016). Potential structuring forces on a shelf edge upper mesophotic coral ecosystem in the US Virgin Islands. *Frontiers in Marine Science*, *3*.

Smith, T.B., Holstein, D.M., & Ennis, R.S. (2019). Disturbance in mesophotic coral ecosystems and linkages to conservation and management. In Y. Loya, K. A. Puglise, & T. C. L. Bridge (Eds.), *Mesophotic Coral Ecosystems* (Vol. 12, pp. 911–929). Springer International Publishing.

Solan, M., & Whiteley, N.M. (Eds.). (2016). *Stressors in the marine environment: Physiological and ecological responses; societal implications* (First edition). Oxford University Press.

Spalding, M.D., & Brown, B.E. (2015). Warm-water coral reefs and climate change. *Science*, *350*(6262), 769–771.

Steffensen, J.F. (1989). Some errors in respirometry of aquatic breathers: How to avoid and correct for them. *Fish Physiology and Biochemistry*, *6*(1), 49–59.

Stuhr, M., Reymond, C.E., Rieder, V., Hallock, P., Rahnenführer, J., Westphal, H., & Kucera, M. (2017). Reef calcifiers are adapted to episodic heat stress but vulnerable to sustained warming. *PLOS ONE*, *12*(7), e0179753.

919 Suarez, H.N., Dy, D.T., & Violanda, R.R. (2015). Density of Associated Macrofauna of Black Corals
920 (Anthozoa: Antipatharia) in Jagna, Bohol, Central Philippines. *Philipp J Sci, 144*(2): 107-115.
921 Svendsen, M.B.S., Bushnell, P.G., & Steffensen, J.F. (2016). Design and setup of intermittent-flow
922 respirometry system for aquatic organisms: How to set up an aquatic respirometry system.
923 *Journal of Fish Biology*, *88*(1), 26–50.
924 Sweetman, A.K., Thurber, A.R., Smith, C.R., Levin, L.A., Mora, C., Wei, C.L., Gooday, A.J., Jones, D.O.B.,
925 Rex, M., Yasuhara, M., Ingels, J., Ruhl, H.A., Frieder, C.A., Danovaro, R., Würzberg, L., Baco, A.,
926 Grupe, B.M., Pasulka, A., Meyer, K.S., & Roberts, J.M. (2017). Major impacts of climate change
927 on deep-sea benthic ecosystems. *Elem Sci Anth*, *5*(0), 4.
928 Szmant, A.M., Ferrer, L.M., & FitzGerald, L.M. (1990). Nitrogen excretion and O:N ratios in reef corals:
929 Evidence for conservation of nitrogen. *Marine Biology*, *104*(1), 119–127.
930 Tazioli, S., Bo, M., Boyer, M., Rotinsulu, H., & Bavestrello, G. (2007). Ecological observations of some
931 common antipatharian corals in the Marine Park of Bunaken (North Sulawesi, Indonesia).
932 *Zoological Studies*, *46*(2), 227-241.
933 Therneau, T.M. (2015a). A package for survival analysis in R. See https://CRAN.R-
934 project.org/package=survival.
935 Therneau, T.M. (2015b). coxme: mixed effects cox models. See
936 https://CRAN.Rproject.org/package=coxme.
937 Thomas, C.J., Bridge, T.C., Figueiredo, J., Deleersnijder, E., & Hanert, E. (2015). Connectivity between
938 submerged and near-sea-surface coral reefs: can submerged reef populations act as refuges?
939 *Diversity and Distributions, 21*(10): 1254–1266.
940 Thurber, R. V., Willner-Hall, D., Rodriguez-Mueller, B., Desnues, C., Edwards, R.A., Angly, F., Dinsdale,
941 E., Kelly, L., & Rohwer, F. (2009). Metagenomic analysis of stressed coral holobionts.
942 *Environmental Microbiology*, *11*(8): 2148–2163.

943 Tsounis, G., Rossi, S., Grigg, R., Santangelo, G., Bramanti, L., & Gili, J.M. (2010). The Exploitation and
944 Conservation of Precious Corals. *Oceanography and marine biology: an annual review, 48*: 161-
945 212.
946 van de Water, J.A., Coppari, M., Enrichetti, F., Ferrier-Pagès, C., & Bo, M. (2020). Local conditions
947 influence the prokaryotic communities associated with the mesophotic black coral
948 *Antipathella subpinnata. Frontiers in Microbiology*, *11*, 2423.
949 Venegas, R.M., Oliver, T., Liu, G., Heron, S.F., Clark, S.J., Pomeroy, N., Young, C., Eakin, C.M., & Brainard,
950 R.E. (2019). The rarity of depth refugia from coral bleaching heat stress in the Western and
951 Central Pacific Islands. *Scientific Reports*, *9*(1), 1-12.
952 Wada, N., Ishimochi, M., Matsui, T., Pollock, F.J., Tang, S.L., Ainsworth, T.D., Willis, B.L., Mano, N., &
953 Bourne, D.G. (2019). Characterization of coral-associated microbial aggregates (CAMAs) within
954 tissues of the coral *Acropora hyacinthus. Scientific Reports, 9*(1): 1-13.
955 Wagner, D. (2015). The spatial distribution of shallow-water (<150 m) black corals (Cnidaria:
956 Antipatharia) in the Hawaiian Archipelago. *Marine Biodiversity Records*, *8*.
957 Wagner, D., Luck, D.G., & Toonen, R.J. (2012). The biology and ecology of black corals (Cnidaria:
958 Anthozoa: Hexacorallia: Antipatharia). In *Advances in Marine Biology* (Vol. 63, pp. 67–132).
959 Elsevier.
960 Wagner, D., Pochon, X., Irwin, L., Toonen, R.J., & Gates, R.D. (2011). Azooxanthellate? Most Hawaiian
961 black corals contain Symbiodinium. *Proceedings of the Royal Society B: Biological Sciences*,
962 *278*(1710), 1323–1328.
963 Wall, M., Putchim, L., Schmidt, G.M., Jantzen, C., Khokiattiwong, S., & Richter, C. (2015). Large-
964 amplitude internal waves benefit corals during thermal stress. *Proceedings of the Royal Society*
965 *B: Biological Sciences*, *282*(1799), 20140650.
966 Wild, C., Huettel, M., Klueter, A., Kremb, S.G., Rasheed, M.Y.M., & Jørgensen, B.B. (2004). Coral mucus
967 functions as an energy carrier and particle trap in the reef ecosystem. *Nature*, *428*(6978), 66–
968 70.

969 Work, T., & Aeby, G. (2014). Microbial aggregates within tissues infect a diversity of corals throughout
970 the Indo-Pacific. *Marine Ecology Progress Series*, *500*, 1–9.
971 Wright, R.M., Strader, M.E., Genuise, H.M., & Matz, M. (2019). Effects of thermal stress on amount,
972 composition, and antibacterial properties of coral mucus. *PeerJ*, *7*, e6849.
973 Wyatt, A.S.J., Leichter, J.J., Toth, L.T., Miyajima, T., Aronson, R.B., & Nagata, T. (2020). Heat
974 accumulation on coral reefs mitigated by internal waves. *Nature Geoscience*, *13*(1), 28–34.
975 Yasuhara, M., & Danovaro, R. (2016). Temperature impacts on deep-sea biodiversity. *Biological*
976 *Reviews*, *91*(2), 275–287.
977 Yesson, C., Bedford, F., Rogers, A.D., & Taylor, M.L. (2017). The global distribution of deep-water
978 Antipatharia habitat. *Deep Sea Research Part II: Topical Studies in Oceanography*, *145*, 79–86.
979 Zhang, X., Sun, Y., Bao, J., He, F., Xu, X., & Qi, S. (2012). Phylogenetic survey and antimicrobial activity
980 of culturable microorganisms associated with the South China Sea black coral *Antipathes*
981 *dichotoma*. *FEMS Microbiology Letters*, *336*(2), 122–130.
982
983

Figure legends

Figure 1. a Photograph of a colony used in the experiment (Scale bar: 3 cm). **b** Close-up photograph of the polypar side of the corallum (Scale bar: 1.5 mm). **c** The healing index (HI), with index from -1 to 5 describing the healing stage of the apical tip of the coral nubbin. Scale bars: HI -1 (10 mm); HI 0 (2 mm); HI 1 (2 mm); HI 2 (1 mm); HI 3 (1 mm) ; HI 4 (1 mm) ; HI 5 (1 mm).

Figure 2. a Annual temperature variability on the North shore of Mo'orea at 3, 25, 35 and 50 m depth (mean ± se, n=1488-4647, by month, data from 2015 to 2021). Figure made from data by SNO Corail from CRIOBE (Tiahura reef site, 17°28.940'S 149° 53.985'W, SBE56 temperature sensors). **b** Variability of temperature (mean temperature per day) over 40 days (9th of October-17th of November 2019) at 6, 20, 40, 60, and 90 m along the outer reef slope studied. Data collected with HOBO Temp V2 data loggers. **c** Temperature variability (5-min interval) at 6, 20, 40, 60, and 90 m showing the activity of internal waves on the 13th of November. Data collected with HOBO Temp V2 data loggers. **d** Radar plot comparing the temperature metrics (described in **e**) at 20, 60 and 90 m during the 40 days of measurements at the study site. The darkness of the blue increases with depth. **e** Quantitative metrics of temperature between depths, between the 9th of October and the 17th of November 2019. Temperature measurements were collected with HOBO Temp V2 data loggers (5-min interval).

Figure 3. Effects of temperature on *Stichopathes sp.* oxygen consumption rate **(a-b)**, ammonium excretion rate **(c-d)** and O:N ratio **(e-f)** after 8 **(a, c, e)** and 16 days **(b, d, f)** of exposure. Points represent the individual nubbins. Curves of **a** and **b** fitted using Two-stage least square regression in the form of a second order polynomial ($y=ax^2+bx+c$) showing 95% confidence intervals. Linear regressions were not significant for **c, d, e** and **f**.

Figure 4. Evolution of the mean healing index (HI) with time, per temperature treatment. Crosses represent the mean healing index of nubbins at each time and temperature treatment (n=8). Lines fitted using ordinal logistic regressions (nonlinear regressions). Greek letters indicate the parameters **α**, **β**, and **γ** of the regression: the mean maximum value of healing index, **α**; the slope (the speed at which α is reached), **β**; and the time at the middle point of the sigmoid, **γ.** Uppercase letters distinguish statistically different groups for each parameter.

Figure 5. Survival plot showing the probability of absence of tissue necrosis with time, per temperature treatment. Uppercase letters indicate statistical differences with the reference group (control treatment, 26°C), using Cox proportional-Hazards Model.

Figure 6. a Linear least-squares regression showing relative surface (%) occupied by mucocytes in tentacles cross-section according to temperature, after 16 days. Data was averaged by nubbins (grey dots). **b-c** Histological cross-section through the tentacle of a polyp, showing the mucocyte cells (arrows) inside the ectoderm, in a polyp at control temperature (**b**) and after 16 days under 30.5°C (**c**). E, ectoderm; M, mesoglea; G, gastroderm; C, CAMAs (Cell-Associated Microbial Aggregates).

Figure 7. Total antioxidant capacity (TAC, expressed in mM Copper Reducing Equivalents per g of protein) according to temperature, after 16 days.

Figure 8. Present (black curve) and extrapolated (+1°C, grey curve) environmental temperatures variations at 90 m (HOBO, 5-min intervals) compared to the thermal optimum for respiration (T_{opt}). Black dotted line indicates the present mean environmental temperature measured over the 40-days period. Grey dotted line indicates the extrapolated mean environmental temperature expected if it increases by one degree.

Table 1. Physico-chemical parameters in the five experimental treatments and on the site of collection.

Treatment (°C)	Salinity	Temperature (°C)	Total alkalinity (µmol kg^{-1})	pH_T
30.5	34.55 ± 0.50	30.10 ± 0.55	2390 ± 6	7.99 ± 0.01
29	34.86 ± 0.15	28.68 ± 0.34	2389 ± 7	8.00 ± 0.01
27.5	33.87 ± 0.39	27.35 ± 0.33	2403 ± 10	8.00 ± 0.01
26	34.56 ± 0.40	26.18 ± 0.20	2391 ± 7	8.02 ± 0.01
26	34.74 ± 0.44	26.22 ± 0.23	2392 ± 7	8.02 ± 0.01
in situ (80m)	34.6	26.74	2354	8.04

Data are means ± standard error. n=16 for salinity and pH_T, n=36-48 for alkalinity, n=3744 for temperature. For in situ data (Niskins bottles): n=2 and only means are therefore reported.

Table 1. Q_{10} values at day 8 and 16 showing the changes in oxygen consumption rates between consecutive temperature treatments.

Temperature change (°C)	Q_{10} day 8	Q_{10} day 16
26 - 27.5	4.78	47.05
27.5 - 29	18.54	0.68

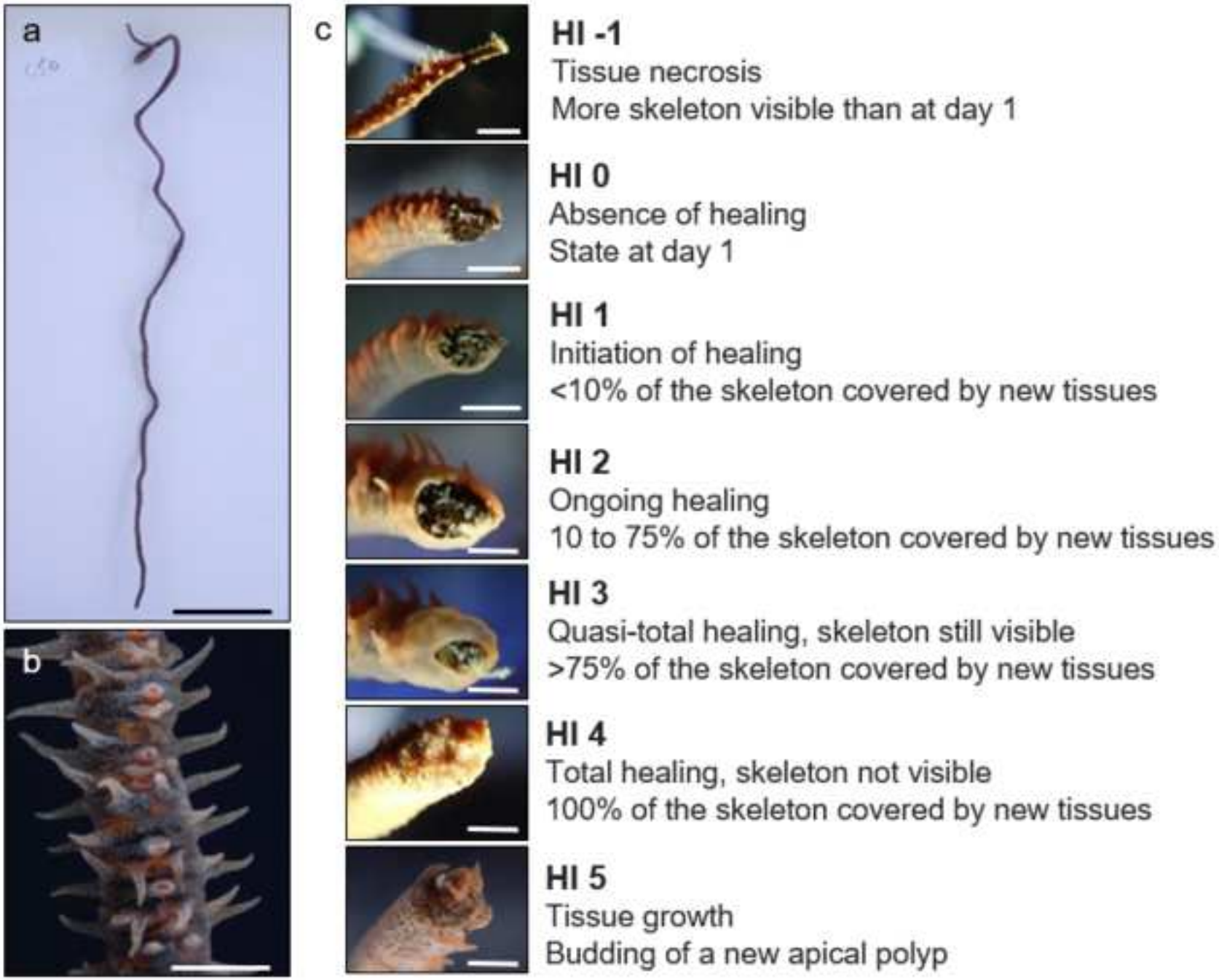

Figure2

Click here to access/download;Figure;Figure2_Godefroid et al..png

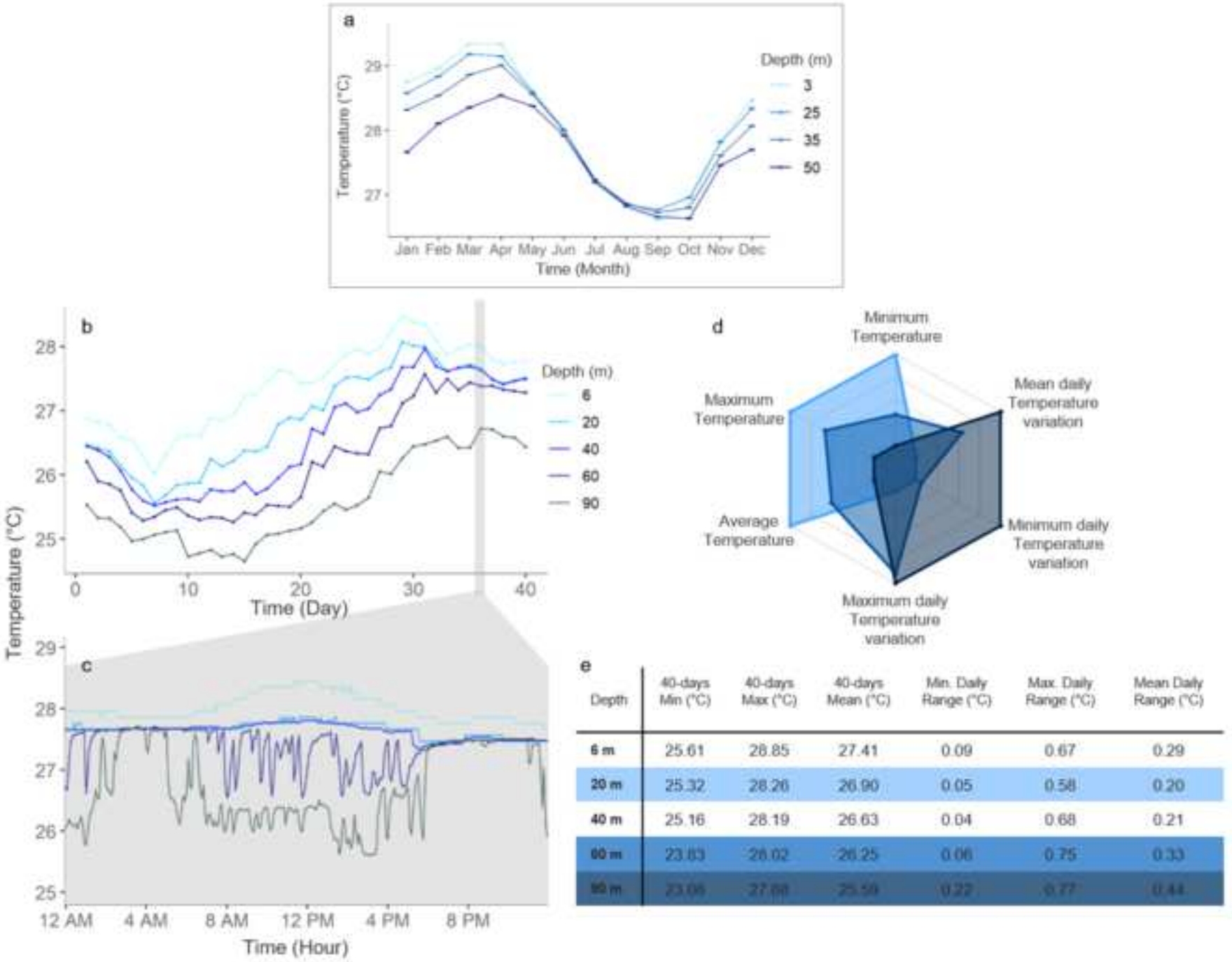

Depth	40-days Min (°C)	40-days Max (°C)	40-days Mean (°C)	Min. Daily Range (°C)	Max. Daily Range (°C)	Mean Daily Range (°C)
6 m	25.61	28.85	27.41	0.09	0.67	0.29
20 m	25.32	28.26	26.90	0.05	0.58	0.20
40 m	25.16	28.19	26.63	0.04	0.68	0.21
60 m	23.83	28.02	26.25	0.06	0.75	0.33
90 m	23.06	27.68	25.59	0.22	0.77	0.44

Figure3

Click here to access/download;Figure;Figure3_Godefroid et al..png

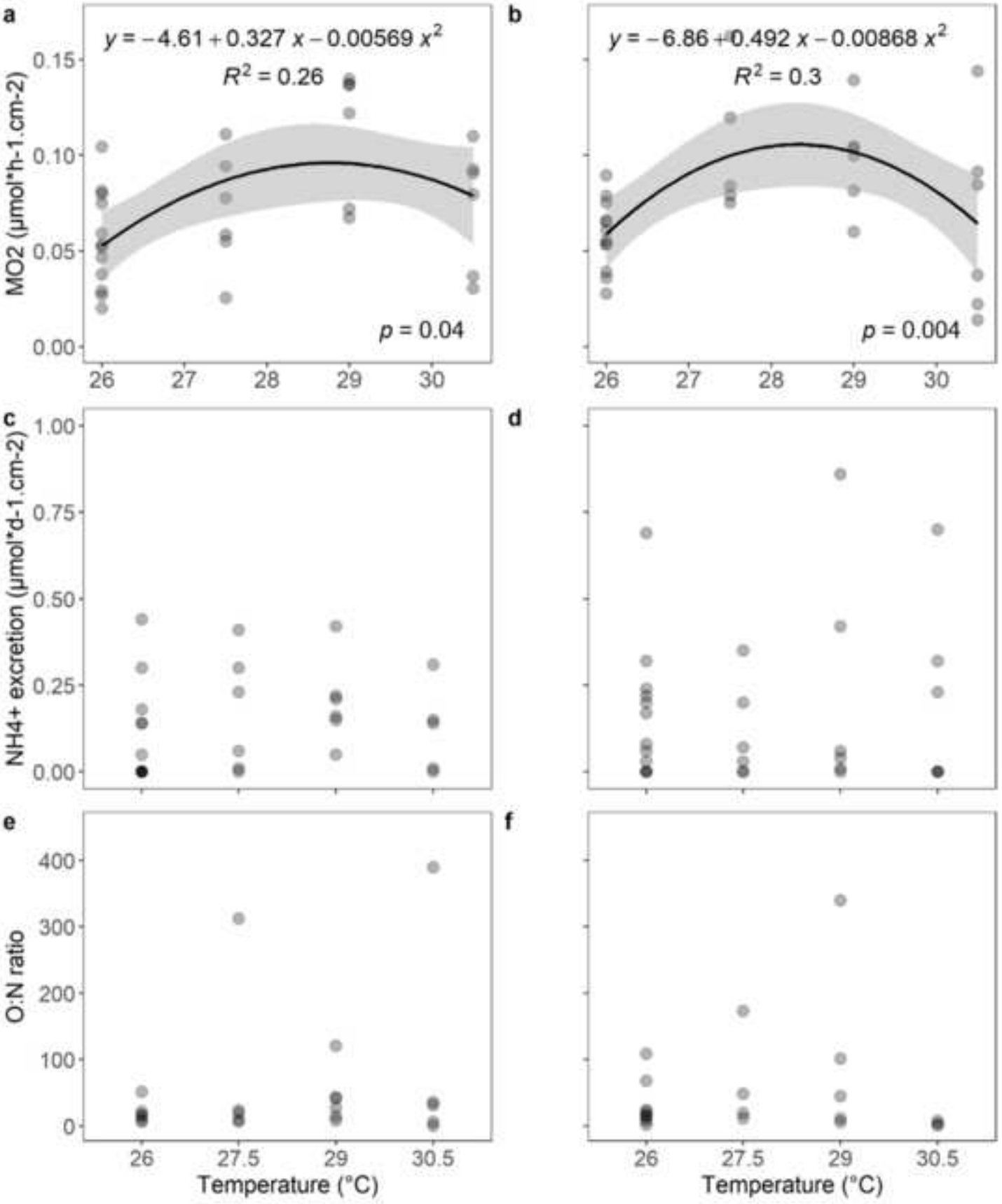

Figure4

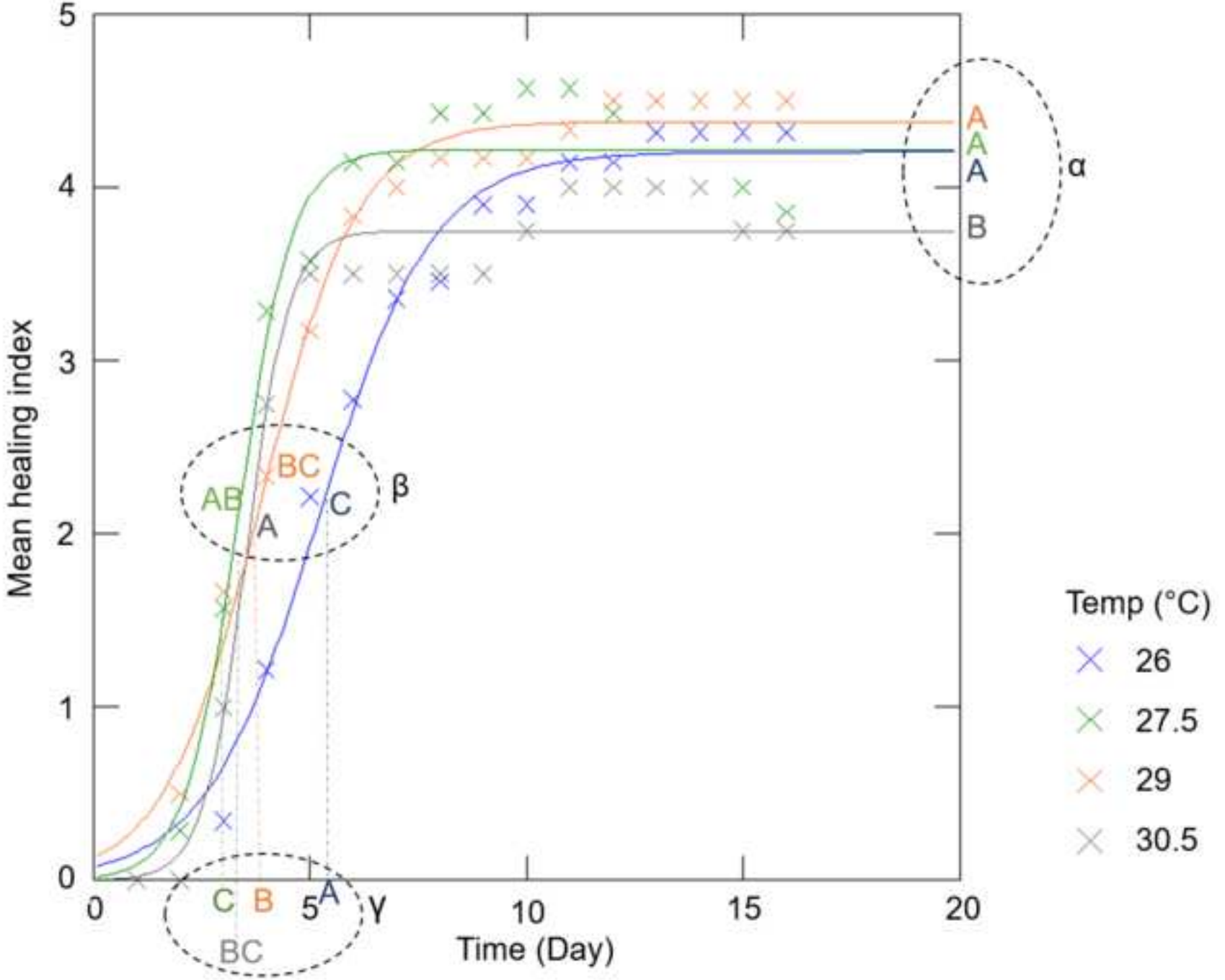

Figure5

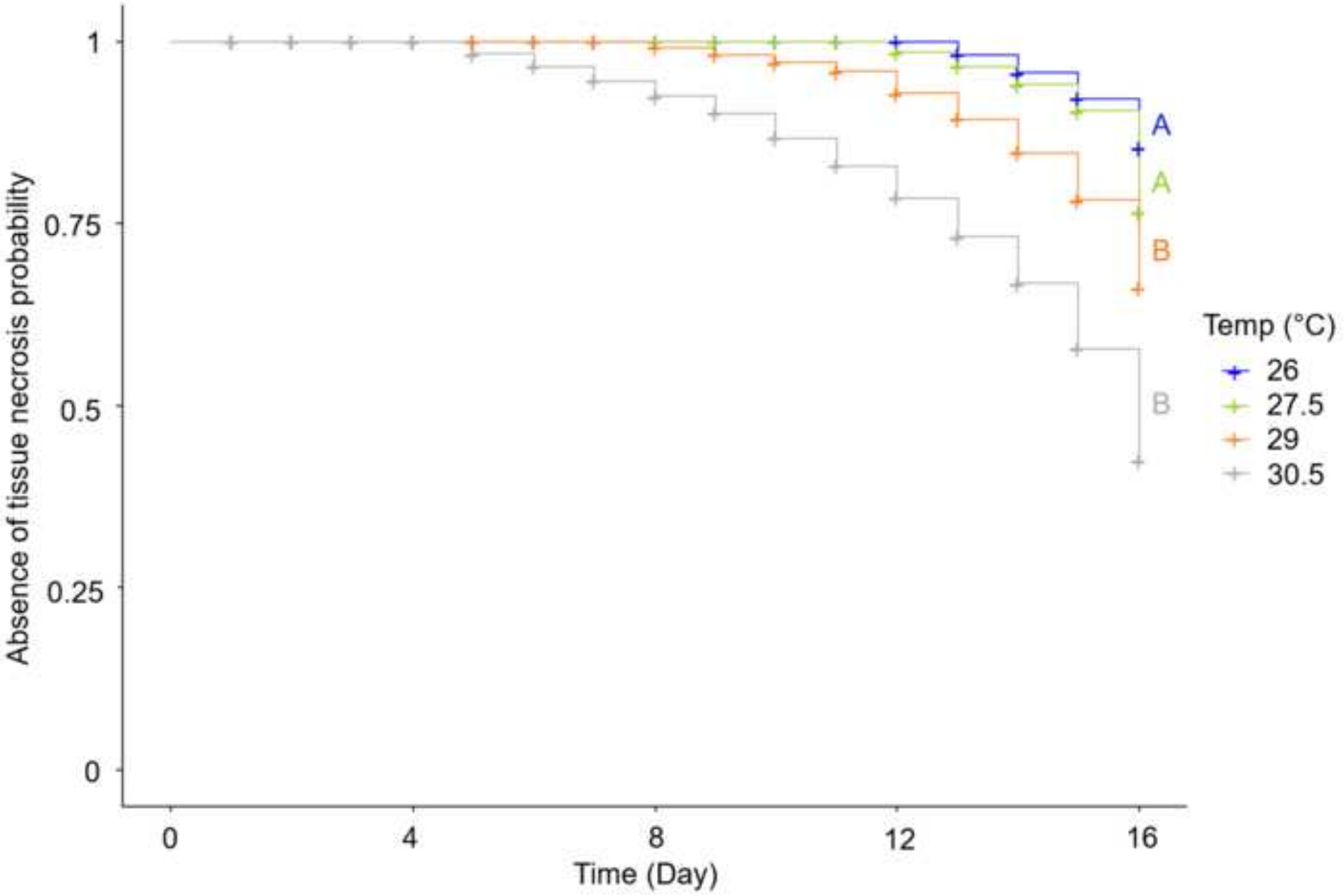

Figure7

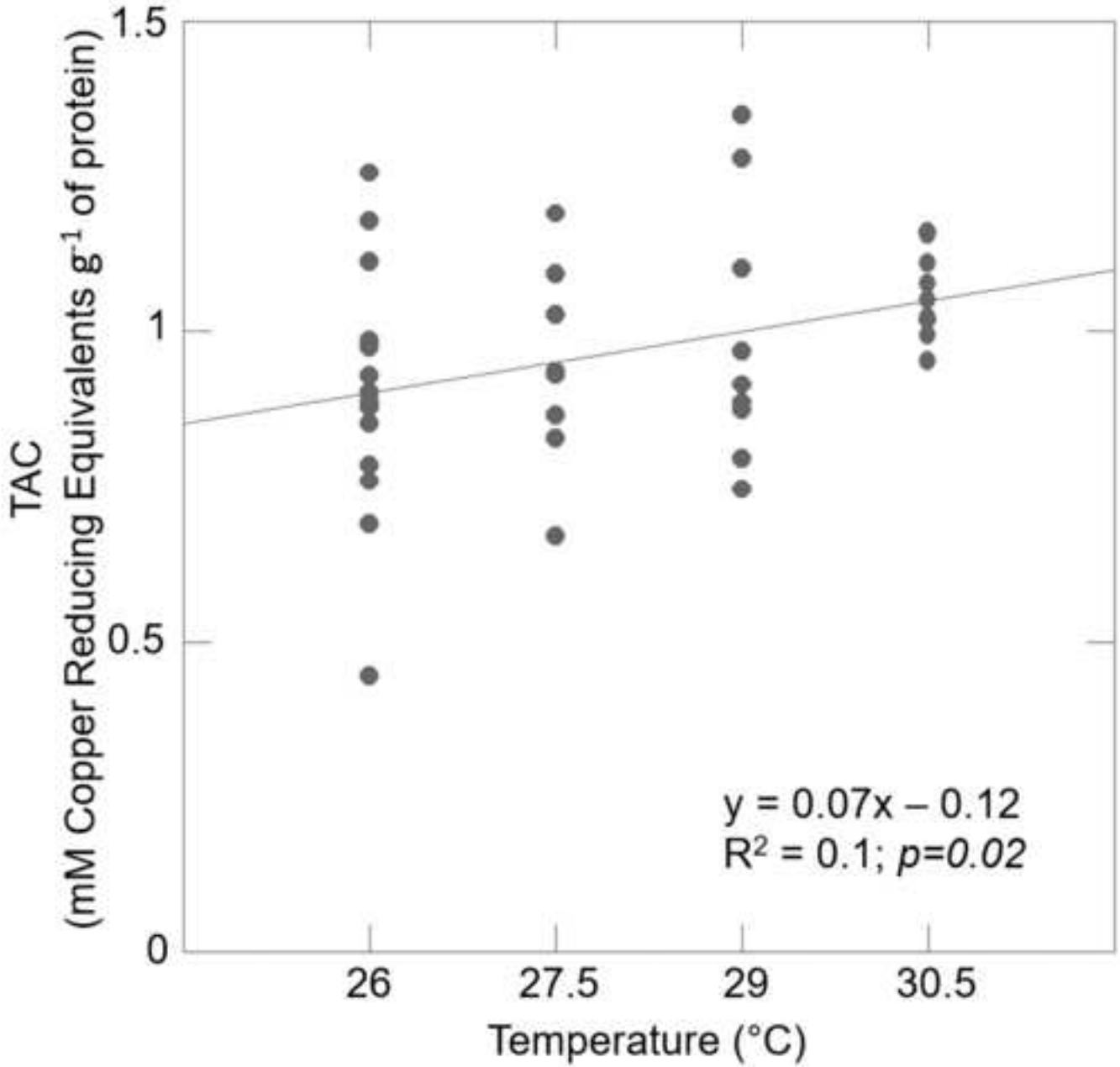

Figure8

Click here to access/download;Figure;Figure8_Godefroid et al.png

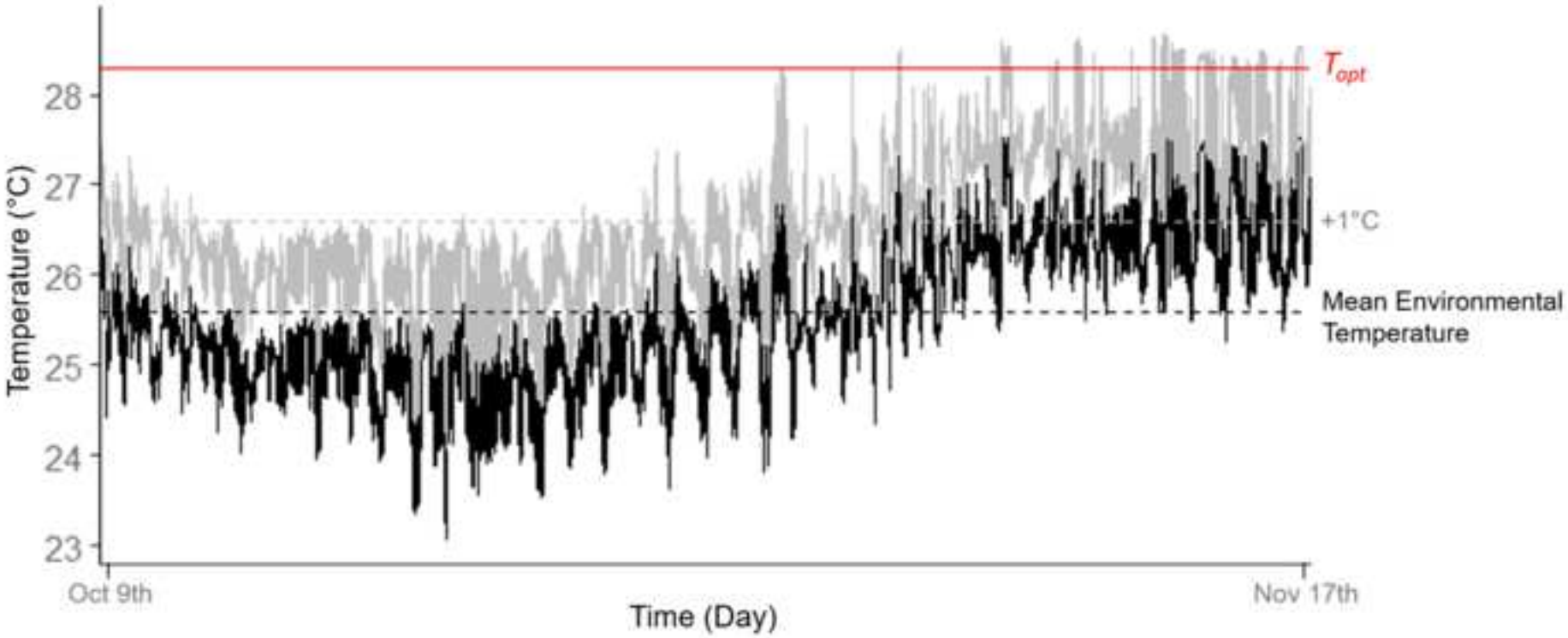

Figure6

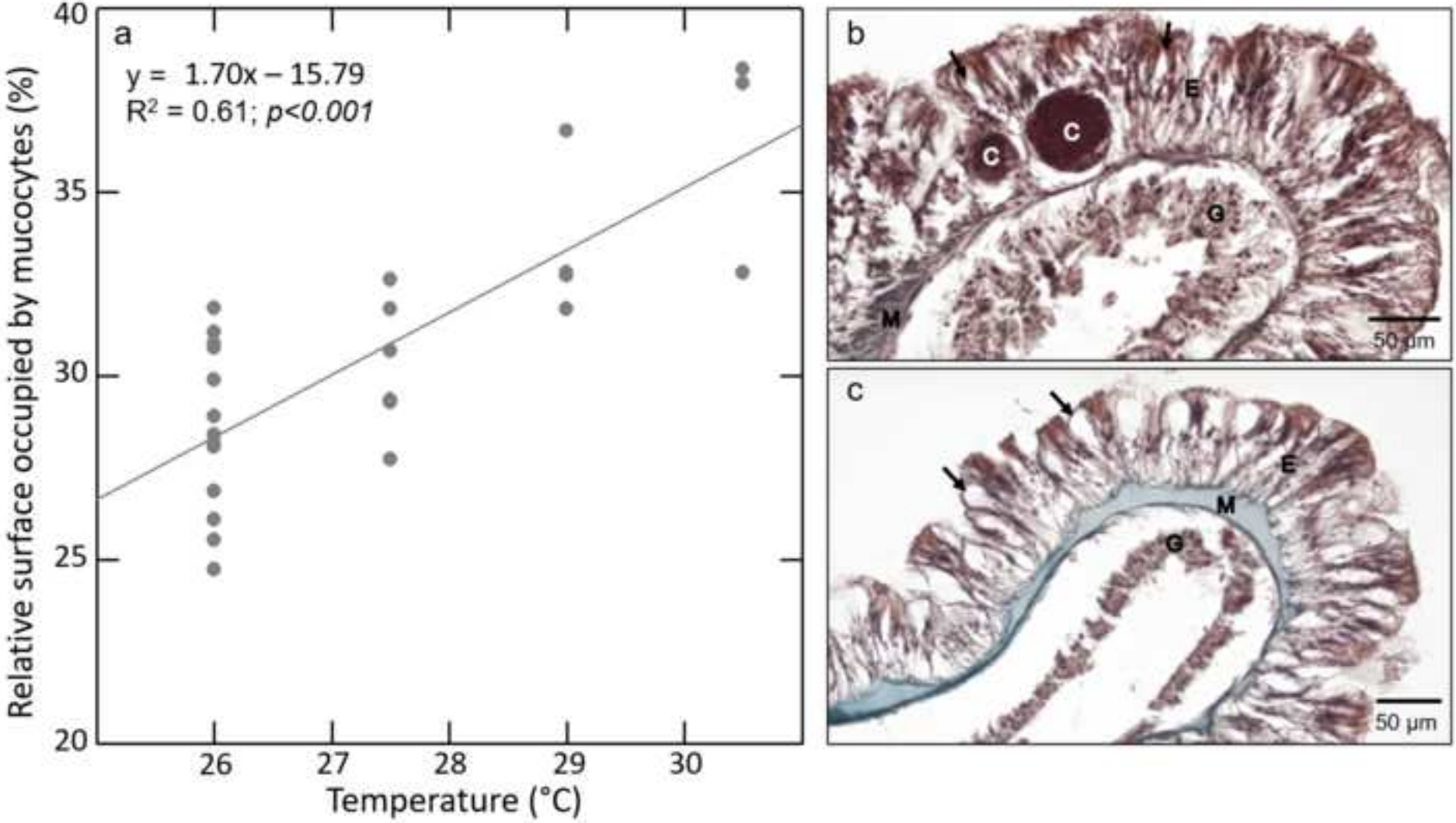

Declaration of interests

☒ The authors declare that they have no known competing financial interests or personal relationships that could have appeared to influence the work reported in this paper.

☐The authors declare the following financial interests/personal relationships which may be considered as potential competing interests:

Credit author statement

Mathilde Godefroid: Conceptualization, Methodology, Formal analysis, Investigation, Writing – Original Draft, Visualisation **Laetitia Hédouin:** Conceptualization, Methodology, Resources, Writing – Review & Editing **Alexandre Mercière:** Software, Resources **Under The Pole Consortium:** Resources **Philippe Dubois:** Conceptualization, Methodology, Resources, Writing – Review & Editing